

Berichte

zur Polar-
und Meeresforschung

614
2010

**Reports
on Polar and Marine Research**



**The Expedition of the Research Vessel "Polarstern"
to the Antarctic in 2009 (ANT-XXVI/1)**

**Edited by
Saad el Naggari and Andreas Macke
with contributions of the participants**

 **HELMHOLTZ
| GEMEINSCHAFT**

ALFRED-WEGENER-INSTITUT FÜR
POLAR- UND MEERESFORSCHUNG
In der Helmholtz-Gemeinschaft
D-27570 BREMERHAVEN
Bundesrepublik Deutschland

ISSN 1866-3192

Hinweis

Die Berichte zur Polar- und Meeresforschung werden vom Alfred-Wegener-Institut für Polar- und Meeresforschung in Bremerhaven* in unregelmäßiger Abfolge herausgegeben.

Sie enthalten Beschreibungen und Ergebnisse der vom Institut (AWI) oder mit seiner Unterstützung durchgeführten Forschungsarbeiten in den Polargebieten und in den Meeren.

Es werden veröffentlicht:

- Expeditionsberichte (inkl. Stationslisten und Routenkarten)
- Expeditionsergebnisse (inkl. Dissertationen)
- wissenschaftliche Ergebnisse der Antarktis-Stationen und anderer Forschungs-Stationen des AWI
- Berichte wissenschaftlicher Tagungen

Die Beiträge geben nicht notwendigerweise die Auffassung des Instituts wieder.

Notice

The Reports on Polar and Marine Research are issued by the Alfred Wegener Institute for Polar and Marine Research in Bremerhaven*, Federal Republic of Germany. They appear in irregular intervals.

They contain descriptions and results of investigations in polar regions and in the seas either conducted by the Institute (AWI) or with its support.

The following items are published:

- expedition reports (incl. station lists and route maps)
- expedition results (incl. Ph.D. theses)
- scientific results of the Antarctic stations and of other AWI research stations
- reports on scientific meetings

The papers contained in the Reports do not necessarily reflect the opinion of the Institute.

The „Berichte zur Polar- und Meeresforschung“
continue the former „Berichte zur Polarforschung“

* Anschrift / Address

Alfred-Wegener-Institut
für Polar- und Meeresforschung
D-27570 Bremerhaven
Germany
www.awi.de

Editor in charge:
Dr. Horst Bornemann

Assistant editor:
Birgit Chiaventone

Die "Berichte zur Polar- und Meeresforschung" (ISSN 1866-3192) werden ab 2008 ausschließlich als Open-Access-Publikation herausgegeben (URL: <http://epic.awi.de>).

Since 2008 the "Reports on Polar and Marine Research" (ISSN 1866-3192) are only available as web based open-access-publications (URL: <http://epic.awi.de>)

The Expedition of the Research Vessel "Polarstern" to the Antarctic in 2009 (ANT-XXVI/1)

**Edited by
Saad El Naggar and Andreas Macke
with contributions of the participants**

**Please cite or link this item using the identifier
hdl:10013/epic.35280 or <http://hdl.handle.net/10013/epic.35280>**

ISSN 1866-3192

ANT-XXVI/1

16 October 2009 - 25 November 2009

Bremerhaven - Punta Arenas

Chief scientists

Saad El Naggari / Andreas Macke

Coordinator

Eberhard Fahrbach

CONTENTS

1. Zusammenfassung und Fahrtverlauf	3
Itinerary and Summary	5
2. Weather conditions	8
3. Autonomous measurement platforms for energy and material exchange between ocean and atmosphere (OCEANET): Atmosphere	13
4. Abyssal temperature fluctuations in the Vema Channel	31
5. Test of a 25.1 mm umbilical cable installed on the mobile Meteor friction winch on board of <i>Polarstern</i>	35
6. Autonomous measurement platforms for surface ocean biogeochemistry (OCEANET): Ocean	38
7. Sea trial and tests of the fibre optical 18 mm cable (LWL) and the telemetry system	44
8. Sea trial and tests of the upgraded under water navigation system “POSIDONIA“	45
9. Occurrence, distribution and isotopic composition of volatile organohalogens along a North-South transect along the Atlantic Ocean	51
10. Aerosol remote sensing with FUBISS sun and sky radiometer	57
11. Diversity and activity of diazotrophic cyanobacteria	60
12. Parasound: system testing and training under expedition conditions – installation of video grab and MSCL	63
13. Acknowledgement	66

APPENDIX

A.1 Teilnehmende Institute / participating institutions	68
A.2 Fahrtteilnehmer / cruise participants	70
A.3 Schiffsbesatzung / ship's crew	71
A.4 Stationsliste / station list PS 75	73

1. ZUSAMMENFASSUNG UND FAHRTVERLAUF

Andreas Macke
IFM-GEOMAR

Am 16. Oktober 2009 trat FS *Polarstern* die Überfahrt von Bremerhaven nach Punta Arenas an. Die Fahrt wurde zur kontinuierlichen Untersuchung atmosphärischer und ozeanischer Eigenschaften sowie der Energie- und Stoffflüsse zwischen Ozean und Atmosphäre im Rahmen der folgenden Projekte genutzt.

Autonome Messplattformen zur Bestimmung des Stoff- und Energieaustausches zwischen Ozean und Atmosphäre (OCEANET)

Um die Messung von Stoff- und Energieaustausch zwischen Ozean und Atmosphäre auf eine solide Basis zu stellen, wurde im Rahmen dieses Projektes mittels der Vereinigung der Expertisen des IFM-GEOMAR (CO₂-/O₂-Flüsse, photosynthetischer Status, Energiehaushalt, Fernerkundung), des IfT (Lidarmessungen), des GKSS Forschungszentrums („FerryBox“ und Fernerkundung der marinen Biologie mit ENVISAT/MERIS) und des AWI-Bremerhaven (CO₂-System, marine Infrastruktur von *Polarstern*) die Entwicklung autonomer Messsysteme fortgeführt, die langfristig für den operationellen Betrieb an Bord von Fracht- und Forschungsschiffen vorgesehen sind (Kapitel 3 & 6).

Messung der Temperaturen im Bodenwasser im Vema-Kanal

In diesem Projekt wurden die hochgenauen Temperatur- und Salzgehaltmessungen in der Umgebung des Vema-Kanals fortgeführt, um Veränderungen des nach Norden strömenden Antarktischen Bodenwassers zu erfassen (Kapitel 4).

Test einer mobilen 2 x 20´-Container-Friktionswinde mit einem JDR Lichtwellenleiter- (LWL-) Kabel

Während des Transfers nach Las Palmas an Bord von *Polarstern* wurde eine zu den Meteor-Großgeräten gehörende mobile Hatlapa-Friktionswinde mit einem LWL-Kabel von JDR getestet. Die Winde war mit dem vorhandenen Kabel nicht einsatzfähig. Das Testprogramm diente dazu, die Einsatzfähigkeit von Winde und Kabel wieder herzustellen (Kapitel 5).

Erprobung eines 18-mm-Lichtwellenleiter-Kabels und des telemetrischen Systems

Ein neues 18-mm-Lichtwellenleiter-Kabel sowie die zugehörige Telemetrie sollte unter realistischen Bedingungen auf See getestet werden. Da das Kabel nicht rechtzeitig geliefert wurde, konnte nur das Telemetrie-System getestet werden (Kapitel 7).

Erprobung des erneuerten Unterwassernavigationssystems POSIDONIA

Nach einem ersten operationellen Test des neuen POSIDONIA während ARK-XXIII/1+2 war auf dieser Fahrt eine abschließende Erprobung vorgesehen, die nicht erfolgreich verlief (Kapitel 8).

Vorkommen, Verteilung und isotopische Zusammensetzung von leichtflüchtigen organischen Halogenverbindungen entlang eines Nord-Süd-Schnitts durch den Atlantischen Ozean

Obwohl bekannt ist, dass natürliche Quellen einen nicht zu unterschätzenden Beitrag zum Eintrag von leichtflüchtigen Halogenkohlenwasserstoffen in die Umwelt leisten, ist der Umfang dieses Eintrages noch weitestgehend unbekannt. Während der Überfahrt wurden kontinuierlich die Luft- und Oberflächenwasserkonzentrationen von leichtflüchtigen Halogenkohlenwasserstoffen sowie deren Isotopenverhältnisse bestimmt, um mit Hilfe dieser Daten Erkenntnisse über die Nord-Süd-Verteilung leichtflüchtiger Halogenkohlenwasserstoffe zu gewinnen. Weiterhin sollte die Frage beantwortet werden, ob die Substanzen anthropogenen oder biogenen Ursprungs sind und inwieweit das Vorkommen von flüchtigen Halogenkohlenwasserstoffen in der Atmosphäre und im Oberflächenwasser durch küstennahe Quellen verursacht wird. Die Daten werden dazu dienen, noch fehlende Puzzleteile im Gesamtbild des natürlichen Halogenkohlenwasserstoffeintrages zu erhalten (Kapitel 9).

Aerosolfernerkundung durch das FUBISS-Himmels- und Sonnenradiometer

Die spektral hochauflösenden Sonnenphotometer FUBISS-ASA2 und FUBISS-ZENITH arbeiten im sichtbaren und nahinfraroten Wellenlängenbereich und wurden vorrangig zur Aerosolfernerkundung entlang der Fahrtroute des Schiffs eingesetzt (Kapitel 10).

Diversität und Aktivität diazotropher Cyanobakterien

Proben zur Erfassung von Abundanz, Diversität und Aktivität diazotropher Mikroorganismen sowie Primärproduktionsraten wurden in regelmäßigen Zeitintervallen genommen und konserviert. Im Anschluss an die Fahrt sollen diese Proben mittels molekularbiologischer Methoden sowie analytischer Flow Cytometrie und Massenspektrometrie untersucht werden (Kapitel 11).

Parasound: Systemtest und Training unter Expeditionsbedingungen - Installation des "video grab" und MSCL

Der Multi-Sensor Core Logger (MSCL) wurde für den Einsatz auf ANT-XXVI/2 installiert und kalibriert. Als Teil der studentischen Ausbildung der Graduiertenschule POLMAR erfolgte ein Training von Fahrtteilnehmern in der Bedienung des neuen hüllenmontierten Parasound-Systems P-70 v.

Bei einem Zwischenhalt in Las Palmas wechselte die Fahrtleitung von Saad El Naggaz zu Andreas Macke.

Die Reise endete am 25. November 2009 in Punta Arenas (Chile).

ITINERARY AND SUMMARY

On 16 October 2009, *Polarstern* started its Atlantic crossing from Bremerhaven to Punta Arenas. Continuous investigations of atmospheric and marine properties as well as for energy and material fluxes between ocean and atmosphere were performed during the cruise. Following a list of projects which were carried out:

Autonomous measurement platforms for energy and material exchange between ocean and atmosphere (OCEANET - Atmosphere & Ocean)

In order to provide a solid basis for the monitoring of energy and material exchanges between ocean and atmosphere the development of an autonomous observation system for operational use onboard cargo- and research vessels was carried on. The project is based on a network of expertise from IFM-GEOMAR (CO₂-/O₂-fluxes, photosynthetic status, energy budget, remote sensing), IfT (lidar measurements), the GKSS research centre (ferry box, remote sensing of marine biology with ENVISAT/MERIS) and AWI-Bremerhaven (CO₂-system, marine infrastructure of *Polarstern*) (section 3 & 6).

Abyssal temperature fluctuations in the Vema Channel

The primary objective was to revisit the Vema Sill and Extension sites for additional high precision CTD measurements to observe the variations of the Antarctic Bottom Water flowing in the Vema channel to the north (section 4).

Test of a 25.1 mm umbilical cable installed on the mobile Meteor friction winch on board of *Polarstern*

During the transfer to Las Palmas a test programme of mobile 2 x 20' container Hatlapa friction winch with a JDR umbilical cable was carried out. The mobile winch then was not serviceable with the JDR umbilical cable in its condition at that time. The test programme was aimed to restore the operability of the winch with the JDR cable (section 5).

Sea trial and tests of the fibre optical 18 mm cable (LWL) and the telemetry system

A new 18 mm fibre optical cable as well as the corresponding telemetric system should be tested under realistic sea conditions. However, since the cable did not arrive in time, only the telemetry could be tested (section 7).

Sea trial and tests of the upgraded under water navigation system "POSIDONIA",

Following a first operational sea trial during ARK-XXIII/1+2 a final test was intended to be performed during this cruise but could not be achieved successfully (section 8).

Occurrence, distribution and isotopic composition of volatile organohalogenes along a north-south transect along the Atlantic Ocean

Natural sources have been found to contribute to the input of volatile organohalogenes to the environment. However, information on the extension of the natural contribution is still scarce. During the *Polarstern* cruise the concentrations and isotopic distribution of volatile organohalogenes in air and surface water along a meridional transect were continuously measured.

The data obtained will be used to obtain information on the meridional distribution, on a biogenic or anthropogenic origin and on possible coastal impacts on volatile organohalogen concentrations in seawater and air. It was expected to find the missing pieces in the picture of the environmental natural input of volatile organohalogenes (section 9).

Aerosol remote sensing with FUBISS sun and sky radiometer

The multispectral Vis/NIR sun- and sky-radiometers FUBISS-ASA2 and FUBISS-ZENITH were applied for the remote sensing of aerosols along the ship's path (section 10).

Diversity and activity of diazotrophic cyanobacteria

Samples for the acquisition of abundance, phylogenetic diversity and metabolic activity of diazotrophic microorganisms as well as primary production rates were taken along the meridional transect at regular times. Following the cruise these were analyzed using molecular biological methods as well as analytical flow cytometry and mass spectrometry (section 11).

Parasound: system testing and training under expedition conditions – installation of video grab and MSCL

Cruise participants were trained in the operation of the new hull-mount Parasound system P-70. Student training is part of the POLMAR Graduate School. For the following cruise ANT-XXVI/2 a Multi-Sensor Core Logger (MSCL) was installed and calibrated (section 12).

At a port call to Las Palmas the chief scientist changed from Saad El Nagggar to Andreas Macke.

The cruise ended on 25 November 2009 in Punta Arenas (Chile).

2. WEATHER CONDITIONS

Hartmut Sonnabend
Deutscher Wetterdienst

Polarstern left the harbour of Bremerhaven on 16 Oct 2009 at 9 p.m. to start its transfer to Punta Arenas. Between a small, but intense gale centre with a pressure of 1009 hPa over the Kattegat and a strong high, centred with a pressure of 1039 hPa over Scotland, a sharp air pressure gradient had formed over German Bight and its coastal regions. This constellation caused storm from the north with forces of 8 – 9 Beaufort associated with violent gusts until early afternoon over this region. Fortunately the low moved quickly south-eastward until time of departure, so that the wind decreased gradually when *Polarstern* entered the southern North Sea from northerly to north-easterly gale force 8 at first, down to Beaufort 5 – 6 until the next morning. Correspondingly the swell dropped down from 5 to 3 meters at the same time. During the next 2 days the high weakened and moved from Scotland to northern France and later on towards central Germany favouring *Polarstern's* passage through the Strait of Dover and the English Channel with soft winds, good visibilities and fine weather- and sea conditions.

The ship entered the northern Gulf of Biscay on 19 Oct. In the meantime a large gale centre had reached a position of 55° N 25° W with a minimum air pressure of 972 hPa. The wind increased up to gale force 8 - 9 Beaufort for a few hours when its cold front crossed the cruise line during the night to 20 Oct. Some time after the wind had shifted to westerly directions with forces around 6 Beaufort associated with frequent shower squalls, a very long termed swell from the northwest with significant heights up to 6 - 7 meters reached *Polarstern* northwest of Cape Finisterre in the afternoon of the same day. This swell was generated in the rear of the large gale centre which became stationary southwest of Ireland with a minimum pressure of 972 hPa. Next a small but intense secondary low, embedded into the frontal zone, reached the working area off the coast between Vigo and Porto in the evening of 21 Oct with a minimum pressure of 994 hPa. Under its influence the wind increased rapidly to gale force 8 – 9 and gusts up to 10 Beaufort from southwest, shifting west quickly. The corresponding development of a very rough wind sea of about 4 meters in combination with the still existing north-westerly swell of about 6 meters caused uncomfortable sea conditions for a while. The responsible low tracked eastward towards the Mediterranean Sea rather quickly, followed by a high drifting north-eastward from the sea areas south of the Acores. After having shifted to northwest the wind decreased during the night until next morning significantly, but the north-westerly swell decreased very slowly to 4 - 5 meters. In the early morning of 23 Oct *Polarstern* reached 36.5°N 13°W for carrying out mooring activities. They were

favoured by soft winds from the west, later on southwest and at same time the north-westerly swell decreased until the evening of this day down to 2 – 2.5 meters. After having finished the 24 hours lasting station work successfully, *Polarstern* proceeded towards the Canary Islands under continuing high pressure influence and dominating soft winds. On 25 Oct the extensive cloud coverage of the days before broke up more and more and gave place to longer sunny periods, permitting the use of the rubber boat for scientific light measurements. Soft winds from easterly to northerly directions accompanied *Polarstern* on its final approach to Las Palmas while the north-westerly swell increased up to 2.5 meters temporarily.

For the change of parts of the scientific crew and logistic reasons *Polarstern* put into the harbour of Las Palmas in the morning of 27 Oct. The passage of a weak cold front was responsible for a mainly cloudy day, but the wind remained nearly calm. In the late evening of the same day the cruise was continued towards a location of 20°N 23°W, the starting point for a section along this meridian until the latitude of 20°S. Corresponding with the weak pressure gradient over the region around the Canary Islands, the wind remained very calm whereas the north-westerly swell still persisted with heights around 2.5 meters at first. After a nearly calm and sunny period, while *Polarstern* passed the axis of a high pressure ridge extending from Spain and Northwest Africa towards the Canary Islands, the northeast trade wind set in gradually in the evening of 28 Oct with forces of 3 – 4 Beaufort. Associated with cloudy sky the trade wind decreased along the southern flank of the subtropical high pressure ridge to 4 - 5 Beaufort next day and reached its maximum on 30 and 31 Oct with wind forces of 5 - 6 Beaufort from northeast, but sunny weather again. Almost at the same time *Polarstern* encountered an extensive area of dust-filled air drifting from the Sahara Desert above Mauritania and the Cape Verde Islands west south-westward, causing significant reduce of visibility especially on 31 Oct while the ship passed through the Cape Verde Islands. These conditions improved gradually in the afternoon of 01 Nov in the approach of the Intertropical Convergence Zone (ITCZ) which extended with its axis along about 7° to 8°N. During the early morning of the following day *Polarstern* encountered a convective cloud band a few hours after having passed 10°N with intermittent rain, showers and sheet lightning. The northeast wind breezed up to 6-7 with gusts near gale force 8 Beaufort at times, shifting southeast later on. Nearly 10.1 litres of precipitation per square metre were measured during this event. After this overture the rest of the day appeared overcast with predominating medium high clouds and some light rain at times. The wind became mainly light to moderate, levelling off to the south hemispheric trade wind gradually. Scattered convective clouds with a few light showers in the vicinity of the ship dominated on 3 Nov while *Polarstern* passed the latitude of 5°N. The water temperatures reached their cruise-maximum of 28.8°C between 14.6°N and 4.3°N on 3 Nov. During the next days the southeast trade wind blew nearly steadily with 5 Beaufort, associated by a south-easterly swell of about 2 meters. Weather conditions were constantly changing between stronger cloud coverage with some light showers and longer periods of sunshine. *Polarstern* reached the equator in the morning of 5 Nov, where it had a nearly 3 hours lasting meeting with the German research vessel

Meteor which operated also in that region. A rubber boat shuttle for mutual visits was arranged between both ships.

Approaching the northern flank of the subtropical high pressure belt, located between 20 and 30°S, meteorological conditions were determined by prevailing easterly trade winds during *Polarstern's* further cruise along 23°W. The wind forces varied between Beaufort 3 – 5 predominantly. Except 8 Nov when it was sunny throughout the whole day, the change between cloudy sky with some light rain showers mainly in the morning and longer sunny periods from noon until evening carried on during the next days.

The end point of the section along 23°W was reached in the afternoon of 10 Nov. From there *Polarstern* continued its course south-westward towards the Vema Channel. A long termed swell reached the ship during the night to 11 Nov rising up to a height of 2.5 meters throughout this day. Meanwhile the moderate to fresh easterly trade wind shifted northeast gradually along the northwest flank of the subtropical high and one day later to north and northwest, when the ship approached to a shallow trough, that extended with its frontal cloud band from the coast of Brasilia between Rio de Janeiro and Sao Paulo towards the latitude of 30°S and from there furthermore eastward. Within the area of this flat trough the weather was often cloudy with some light showers during the next 2 days, while sunny periods were frequently observed in the afternoon. The wind blew predominantly soft to moderate from different directions apart from 13 Nov when these conditions were interrupted by a fresh breeze from northwest around noon. On 15 Nov a flat trough passed a little bit south of *Polarstern's* cruise line causing drizzle at times and light showers. The wind became fresh to strong and shifted from northwest in the morning to south and southeast in the evening. The next day, when a new high pressure cell approached from the mouth of Rio de la Plata was mainly sunny, but with wind forces between 5 and 6 Beaufort from south southwest still windy and chilly as air temperatures dropped down to 17°C. In the early morning of 17 Nov *Polarstern* crossed the centre of the high with soft winds for some hours. In front of an approaching frontal system belonging to a gale centre which moved from Patagonia towards the Falkland Islands, the wind shifted to north, increasing to 5-6 Beaufort in the afternoon of the same day, and up to Beaufort 7, gusts 8 during the night to the following day. After the passage of the cold front the wind shifted south and later on east, calming down soon. Until the evening of this day the sky was overcast by medium high clouds with some light rain at times. In the evening of the same day the ship encountered a south-westerly swell up to 3 meters.

While carrying out station work around 40°S 50.5°W in the morning of 19 Nov a quickly intensifying low, coming from Uruguay, passed hardly northeast and east of these coordinates causing overcast sky and rain for several hours. At same time the wind freshened up to 7-8 Beaufort from northeast, shifting east to southeast later on. Entering into a small high pressure ridge the wind decreased soon in the evening of this day, shifting to northwest during the following night. Along the northeast flank of a large low pressure system extending from the western part of the Drake Passage

towards Fireland flat troughs and high pressure ridges passed the cruise line of *Polarstern* throughout the next days. On 21 Nov the weather was sunny with northwesterly winds around 5-6 Beaufort. Next day the cold front of a low moving from the Falkland Islands towards Elephant Island crossed the cruise track with northerly winds of 6-7 Beaufort on its front side for some hours. As the centre of the low pressure system tracked into the northern Weddell Sea, the fresh to moderate wind shifted to westerly and south-westerly directions gradually, increasing a little bit to Beaufort 6 during the night to 23 Nov. Influenced by a new high pressure cell which moved from Patagonia eastward, the wind decreased to a moderate breeze from southwest and northwest later on throughout *Polarstern's* final approach to the Strait of Magellan. During the last section through the Strait of Magellan to Punta Arenas the frontal trough of a low pressure system west of the Antarctic Peninsula and Fireland caused strong westerly to north-westerly winds. *Polarstern* reached berth of Punta Arenas in the morning of 25 Nov 2009.

The following diagrams show the vertical profiles of temperature (Fig. 2.1), zonal wind (Fig. 2.2), and meridional wind (Fig. 2.3) along the cruise from the daily 12:00 UTC radiosonde ascents.

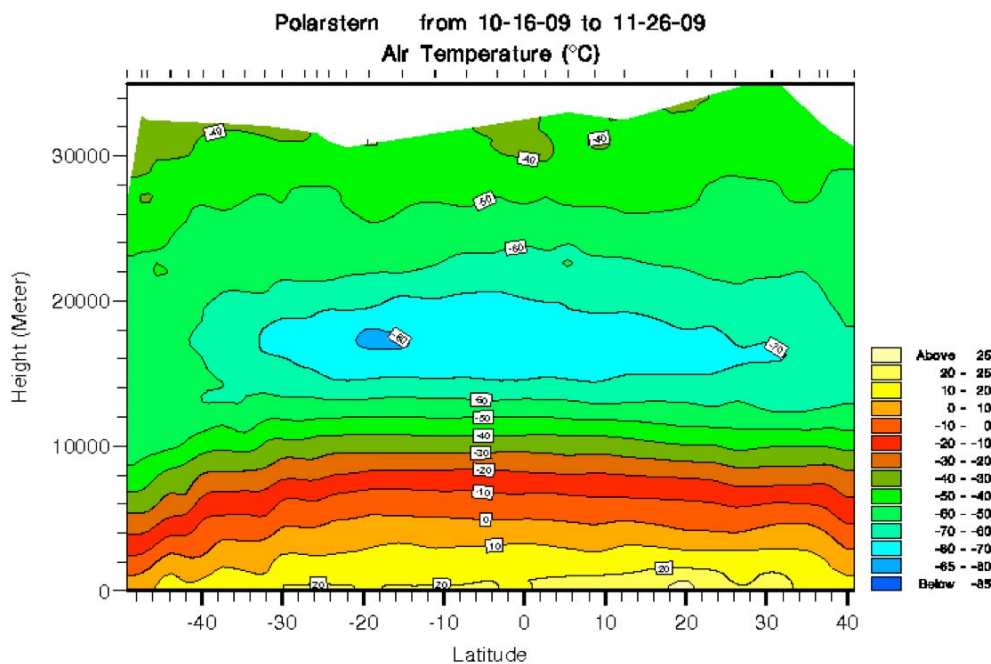


Fig. 2.1: Vertical profile of temperature along the cruise from the daily 12:00 UTC radiosonde ascents. Graphic by Gert König-Langlo

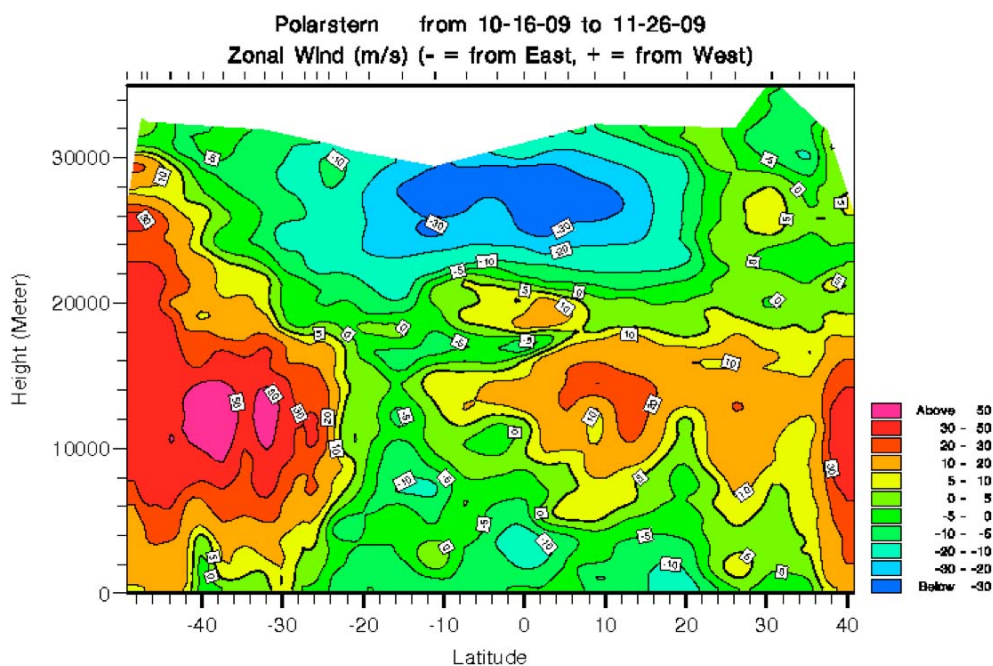


Fig. 2.2: Vertical profile of zonal wind along the cruise from the daily 12:00 UTC radiosonde ascents. Graphic by Gert König-Langlo

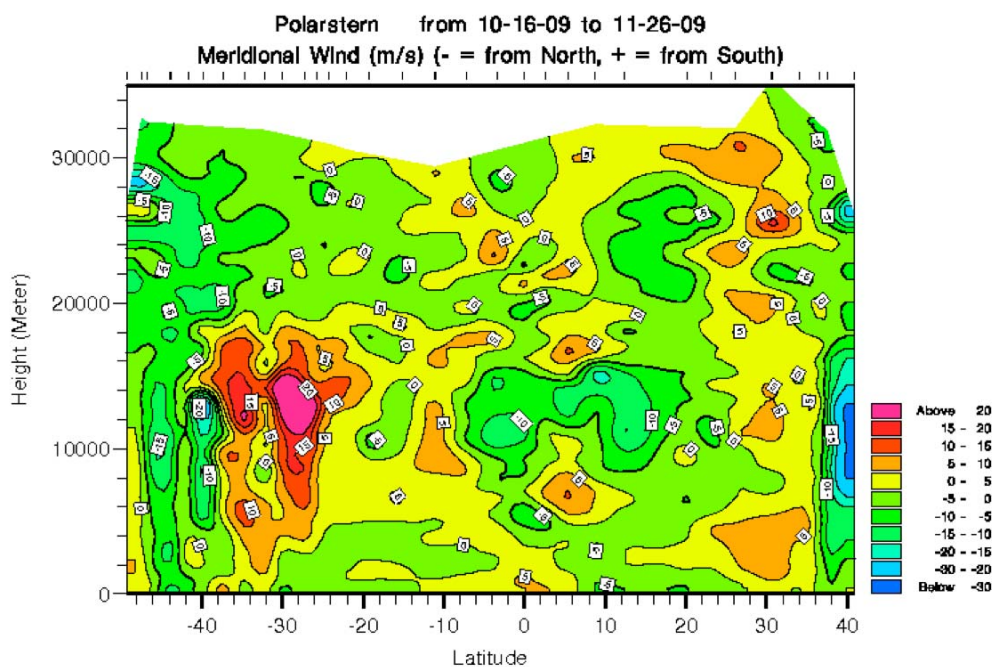


Fig. 2.3: Vertical profile of meridional wind along the cruise from the daily 12:00 UTC radiosonde ascents. Graphic by Gert König-Langlo

3. AUTONOMOUS MEASUREMENT PLATFORMS FOR ENERGY AND MATERIAL EXCHANGE BETWEEN OCEAN AND ATMOSPHERE (OCEANET): ATMOSPHERE

Andreas Macke¹, Karl Bumke¹, John Kalisch¹, Martin Hieronymi¹, Yann Zoll¹, Thomas Kanitz², Jonas von Bismarck³, Marco Starace³, Thijs Heus⁴, Henry Kleta⁵
not on board: Dietrich Althausen², Thomas Ruhtz³

¹IFM-GEOMAR

²IfT

³IfW-FU-Berlin

⁴ZMAW

⁵DWD

Objectives

Clouds remain one of the biggest obstacles in our understanding of the coupled ocean-atmosphere climate system. Even under realistic forcing from observed wind, humidity and pressure fields climate models have difficulties to reproduce the correct spatial and temporal climatology of cloud cover. Because of the strong inhomogeneity of cloud pattern on those scales that are relevant for the radiative transfer processes it is clear that subgrid-scale processes must be accounted for in radiative transfer parametrizations. Combined observations of cloud physical and radiative properties are a key to adjust or to validate such parameterizations.

The turbulent fluxes of heat, momentum, humidity and CO₂ are measured to close the energy and mass budget at the sea surface. Most measurements are part of the Leibniz network-project OCEANET. Within this project the OCEANET-Atmosphere observatory, a 20-foot sea container equipped with *in-situ* and remote sensing instruments has been developed and is applied on this cruise for the first time (see Fig. 3.1). A new instrument in OCEANET-Atmosphere is the Polly lidar system from IfT for vertical profiling of aerosol and cirrus clouds. These measurements are accompanied by regular sun photometer observations of aerosol properties that are performed for the Marine Aeronet Network MAN operated by NASA.

A further and related goal is to quantify the role of clouds and sea surface wave on the small scale temporal and spatial variability of the solar radiation below the sea surface.



Fig. 3.1: The OCEANET-Atmosphere observatory on its first task. Photograph by Jonas von Bismarck

Work at sea

After lifting the OCEANET-Atmosphere container onto the observation deck in Bremerhaven all instruments have been launched while *Polarstern* was still at the Pier. The OCEANET-Atmosphere container comprises the following instruments (bold letters):

The upward looking **pyranometer** Kipp & Zonen CM 21 and the **pyrgeometer** CG 4 operated by IFM-GEOMAR provide the broadband downwelling shortwave radiation (DSR) and the downwelling longwave radiation (DLR) every second.

Every 15 seconds **full sky images** were obtained from a weather proofed digital camera system manufactured at IFM-GEOMAR. This enables a detailed analysis of the role of cloud cover and cloud type on the radiation budget at the sea surface. These images are also valuable for the aerosol remote sensing activities to identify clear sky cases.

As for the previous five Atlantic transects of *Polarstern* a multi-channel **microwave radiometer** (HATPRO, Radiometer Physics) was utilized for continuous observations of atmospheric temperature and humidity profiles as well as liquid water and precipitable water path.

Together with ceilometer measurements of cloud bottom height, sun photometer measurements of aerosol optical thickness, IR radiometer measurements of cloud bottom temperatures, the data from the microwave radiometer provide a unique set of information to interpret the amount of downwelling solar and thermal radiation at the sea surface.

One of the seven humidity channels (the one that is most sensitive to surface-near humidity) malfunctioned at the beginning of the cruise and could not be fixed on board. The instrument consists of 14 channels in total so that the loss of one channel was not dramatic. However, the retrieval algorithm that converts microwave radiation into atmospheric properties needed to be adjusted to the new situation, which required much of the time during the cruise.

For the second time a **Licor** that measures turbulent fluxes of water vapour and CO₂ in combination with a **Metek** sonic anemometer has been installed. An older backup instrument (M100 + sonic anemometer) for observations of turbulent fluctuations of water vapour had been installed in addition of the crows nest. Both instruments were functioning properly during the entire cruise.

Lidar measurements had been performed, whenever weather conditions were appropriate. The system was switched off during midday, when high sun elevations could damage the sensible optics. Also during precipitation and because of a laser hardware failure at the beginning of the transect the measurements had been interrupted.

The used Polly^{XT} that had been developed at the IFT emits laser pulses at 1064, 532 and linear polarized light at 355 nm into the atmosphere and measures the backscattered elastic light at 180° scattering angle. Additionally the Raman method is utilized by detecting molecular scattering of nitrogen at 387 and 607 nm. The opportunity of observing depolarization at 355 nm rounds up the system. The scattered light at each wavelength is measured every 30 s up to 30 km height at a range resolution of 30 m. Thus, it provides the chance of a high temporal and range resolved description of the vertical aerosol distribution.

The analysis of the retrieved optical and microphysical properties allows the characterization of separated aerosol layers with high vertical resolution. In combination with a radiative transfer model the results will help to quantify the solar aerosol radiative forcing above oceans.

As a byproduct Polly^{XT} provides cloud base and top height, the latter for thin clouds only.

Within the OCEANET project a shipborne automatic weather station has been developed. The so called SCalable Automatic Weather Station (**SCAWS**) is based on standard hardware (Campbell Scientific) and measures autonomously the following parameters: time, position, speed and course over ground, heading, barometric

pressure, temperature, rel. humidity, wind (direction and speed) and radiation (short- and longwave). During the cruise the system has been tested under various conditions and has been integrated further more into the OCEANET Atmosphere container and has been prepared to operate fully independently during the following cruises ANT-XXVI/2, 3 and 4 of *Polarstern*. The sensors are standard within the maritime network of DWD. The system provides a complete set of data every second (proprietary NMEA 0183 protocol) and an hourly weather report (FM13 SHIP) which is transmitted ashore via the DWD owned Data Collection Platform (DCP).

In addition to these standard outputs SCAWS monitors the power supply of the sky imager installed on top of the OCEANET-Atmosphere container. This information is included with mean values of the connected radiation sensors and transmitted ashore as well, thus allowing real-time monitoring of the radiation fluxes and the status of the sky imager. It is planned to add further instruments of OCEANET-Atmosphere to SCAWS in the future.

Underwater light measurements have been carried out at the 1 pm board time stations when direct sun was available and sea conditions were suitable for safe zodiac boat operations. Then, three procedures were conducted in parallel. Firstly, a zodiac boat was launched from which an underwater camera device was deployed (see Fig. 3.2). The device that has been developed at the IFM-GEOMAR takes motion pictures of a white plate on which light patterns are mirrored. By means of this method spatiotemporal light field fluctuations in response to undisturbed waves were recorded up to 25 m of water depth. In a second step, a spectral radiometer (RAMSES-ACC-VIS) was lowered from the working deck of the vessel. In order to quantify light fluctuations in the upper layer, two minute long samplings were conducted at defined water depths up to 45 m. For comparison purposes fast lowering measurements up to the same depth were performed. At the same time a CTD was lowered up to 200 m for gaining fluorescence data and thus statements on phytoplankton and turbidity in the water column. Additional data of relevance as sea state parameters and meteorological data are collected as well.



Fig. 3.2: Measurements of subsurface light fluctuations from the zodiac outside the ships sun and wave shadows. Photograph by Martin Hieronymi

The Microtops sun photometer is a handheld device (see Fig. 3.3) to measure water vapour and aerosol optical depth for 5 different wavelengths. The instrument worked without any technical problems, and in comparison with the more advanced spectral radiometers, the Microtops has performed well. While the instrument has the disadvantage that it is a time consuming way of measurement, it has the advantage that it requires hardly any set-up time, meaning that even short spells of clear air can be utilized for measurements.

Fig. 3.3: Thijs Heus operating the Microtops sun photometer. Photograph by Johannes Lampel



Preliminary results

Fig. 3.4 shows the time series of integrated water vapour (IWV) and liquid water path (LWP) along the cruise. The *in-situ* observed IWV from the radiosonde measurements is also shown, and provides a generally good agreement with the indirectly obtained microwave products. Largest water vapour paths of more than 50 gm^{-2} are observed at the thermal equator, where the warm conditions and strong cloud induced upwind pump most humidity from the ocean into the troposphere. The cloud LWP is given by the occasional data points above a background noise, which needs to be corrected for during later analysis. The corrections make use of the sky camera images and upward looking IR-radiometer measurements which indicate clear sky situations above the ship during day time.

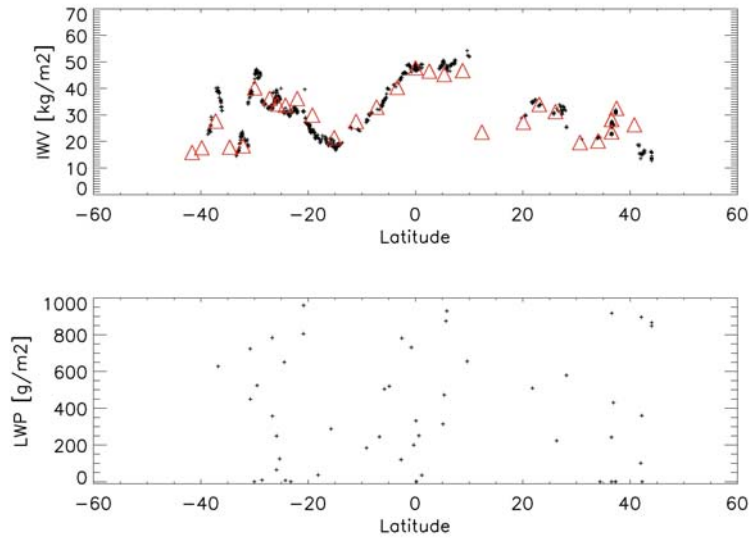


Fig. 3.4: Time series of water vapour path (upper diagram) and liquid water path (lower diagram) from the HATPRO microwave radiometer. The water vapour path from the radiosonde measurements is also shown. Graphics by Yann Zoll

Fig. 3.5 shows the meridional temperature profile along the *Polarstern* cruise. The corresponding humidity profiles are shown in Fig. 3.6. Besides the typical variations caused by the different climate regimes, a Saharan dry air layer advection can be identified around 27°N with warmer temperatures and lower humidity values. As these results are based on an “emergency retrieval” due to the failure of one microwave channel the raw data need to be re-analysed back home after proper recalibration of the microwave radiometer.

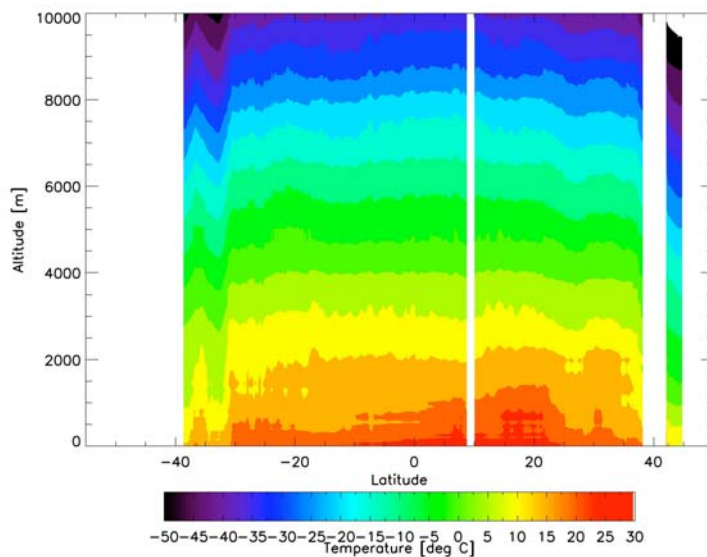


Fig. 3.5: Vertical profiles of temperature retrieved from the microwave radiometer along the cruise track, shown as a function of latitude. Graphics by Yann Zoll

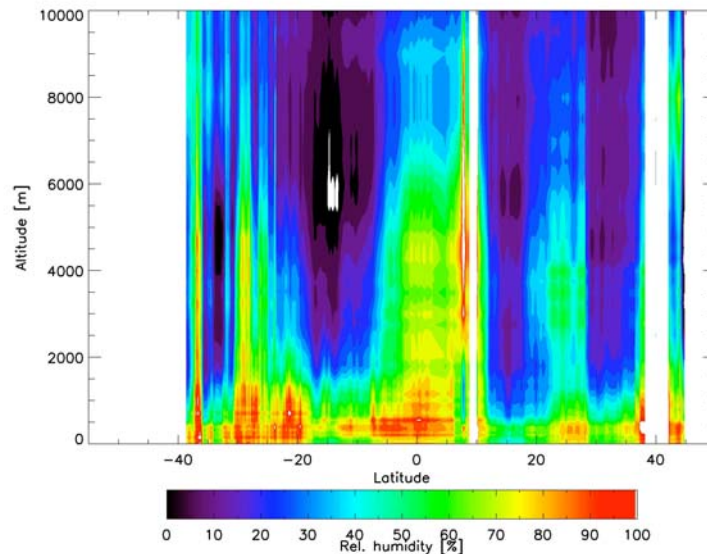


Fig. 3.6: Vertical profiles of relative humidity retrieved from the microwave radiometer along the cruise track, shown as a function of latitude. Graphics by Yann Zoll

The daily time series of the downwelling shortwave and longwave radiation along the entire *Polarstern* cruise are summarized in Fig. 3.7.a-c. For reference, the theoretical curve for clear sky radiation is also shown. Although clouds usually block the sun and reduce the downwelling solar radiation, many occasions of a radiation excess can be found, which is attributed to the increased diffuse downwelling radiation during broken cloud conditions (because of this termed as “broken cloud effect”). Further analysis will test the correlation between the observed cloud properties like cloud cover and liquid water path, and the surface radiation budget. An interesting situation was found on October 31 and November 1 when a Sahara dust layer lead to a nearly constant reduction in the DSR.

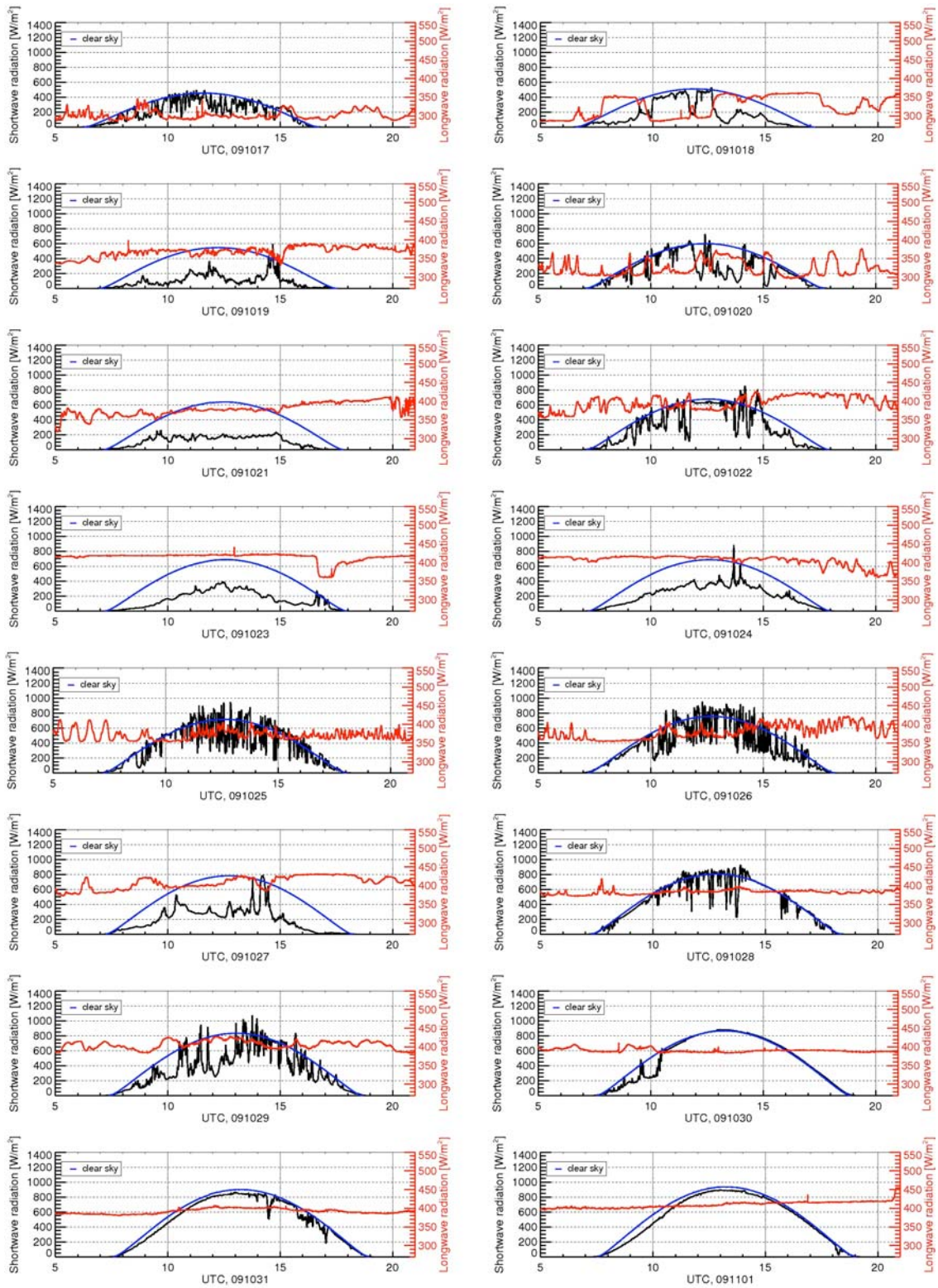


Fig. 3.7a: Daily time series of downwelling broadband solar (black) and thermal (red) radiation from October 17 to November 1, 2009. The reference clear sky radiation (blue) is shown for comparison. Graphics by John Kalisch

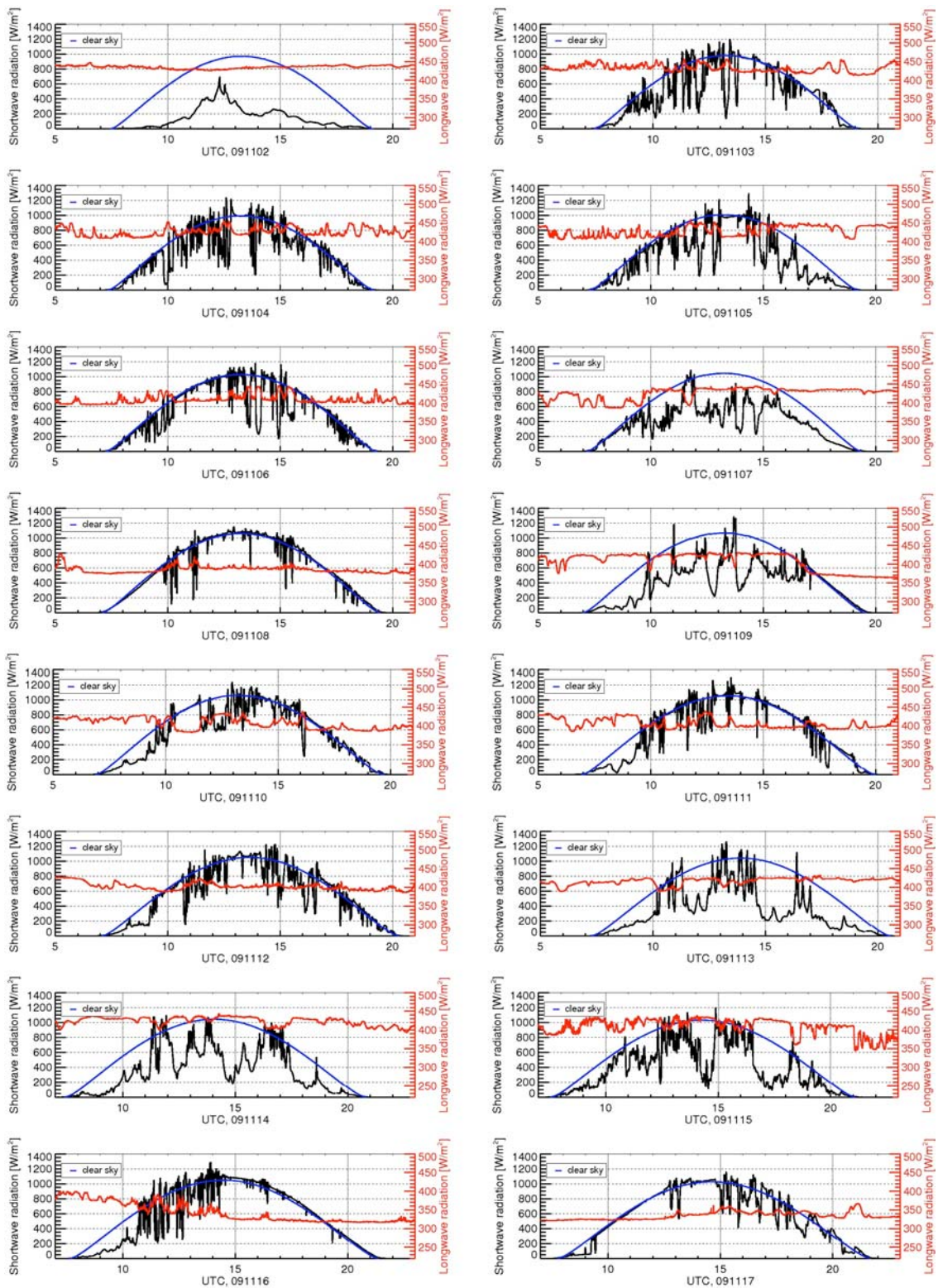


Fig. 3.7b: Daily time series of downwelling broadband solar (black) and thermal (red) radiation from November 2 to November 17, 2009. The reference clear sky radiation (blue) is shown for comparison. Graphics by John Kalisch

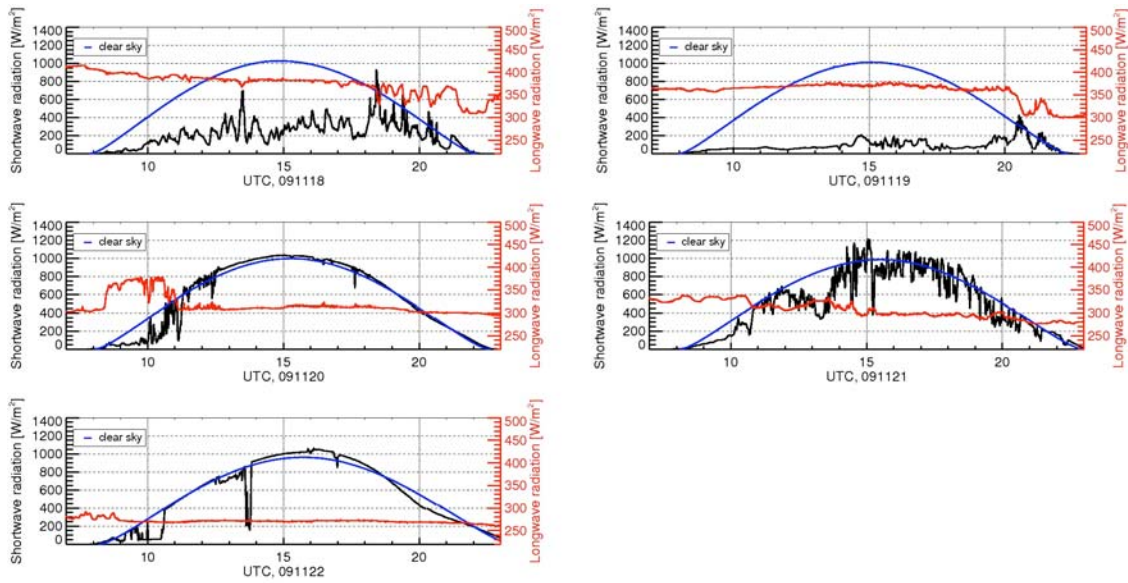


Fig. 3.7c: Daily time series of downwelling broadband solar (black) and thermal (red) radiation from November 18 to November 22, 2009. The reference clear sky radiation (blue) is shown for comparison. Graphics by John Kalisch

During this cruise five situations with exceptionally high solar radiation (larger than 1500 Wm^{-2}) at the surface due to the above mentioned broken-cloud-effect have been recorded. The overall maximum was 1647 Wm^{-2} on 09 Nov 13:16:51 UTC. This is the largest value that we have been observed since the begin of our radiation measurements on *Polarstern* in 2007. Fig. 3.8 shows a one-hour time series capturing this event with high temporal resolution. In comparison to the one-minute averages provided by the operational pyranometer from *Polarstern* the OCEANET pyranometer with 1 second measurement intervals nicely resolves the strong variability of the downwelling radiation. This variability – further enhanced by light focusing/defocusing at the sea surface – may have a significant influence on photo-biological and photo-chemical processes in the upper ocean.

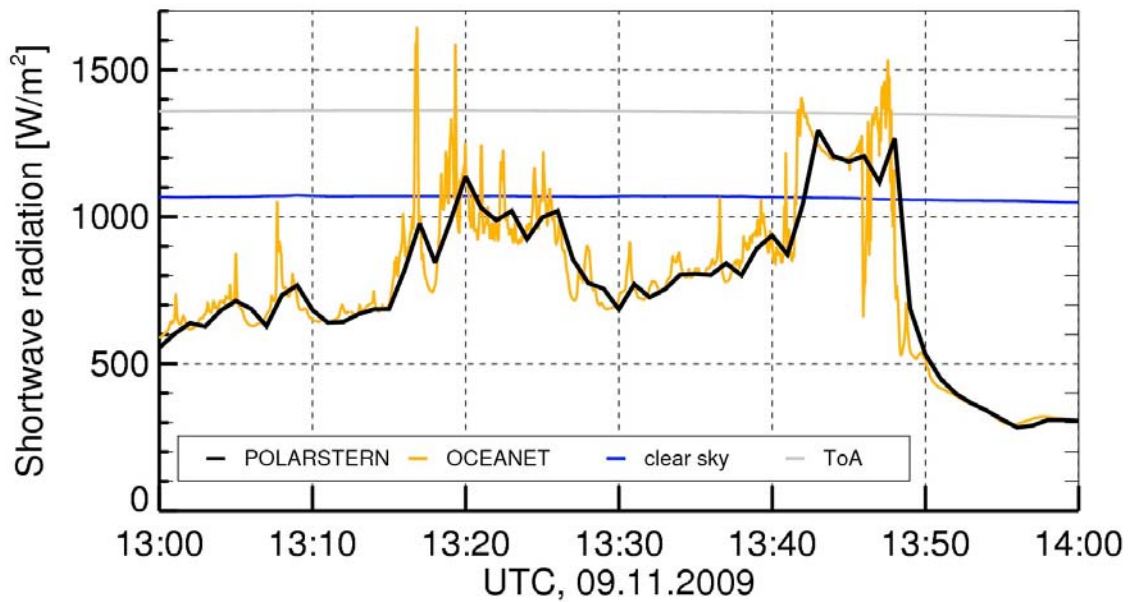


Fig. 3.8: One-hour time series of downwelling shortwave radiation from the Polarstern pyranometer (one minute averages) and the OCEANET pyranometer (1 second intervals). The theoretical curves for top-of-atmosphere flux and clear-sky flux at the surface are also shown. Diagram by John Kalisch

The sky image at the very moment of this occurrence is depicted in Fig. 3.9. It clearly shows that it requires nearly overcast skies with broken alto cumulus clouds where the full solar disk can penetrate through a cloud gap. The additional white diffuse downwelling scattering at the clouds, in particular in the vicinity of the solar disk produces the strong enhancements.



Fig. 3.9: Full sky image during the largest solar downwelling radiation at the surface measured during this cruise. Photograph by John Kalisch

The energy budget at the sea surface is complemented by turbulent fluxes of heat (sensible heat) and the turbulent fluxes of humidity (latent heat). Our direct high frequency measurements of wind, humidity and temperature require a careful quality check and a time consuming numerical analysis before they can be converted into turbulent fluxes. In the meantime, first estimates of these fluxes have been calculated from bulk parameterizations which only require standard meteorological observations. Fig. 3.10 summarizes the total energy balance including all radiation and turbulence terms for most of the cruise. It is interesting to see how close the total budget is to zero despite the large variabilities of the individual terms, especially the solar radiation. Obviously, the thermodynamical system ocean/atmosphere is not too far apart from thermal equilibrium. Still, depending on cloudiness, wind speed, humidity and temperature there are significant net fluxes of energy into or out of the ocean. The thorough analysis of these data back at IFM-GEOMAR will provide important validation points for our climate modellers who are working on ocean/atmosphere interaction.

High frequency measurements of CO₂ concentration have also been taken as well and will be transformed into turbulent CO₂ fluxes. Together with our Ferry-Box observations of the marine CO₂ and its variability, the atmosphere/ocean CO₂ exchange can be investigated in more detail.

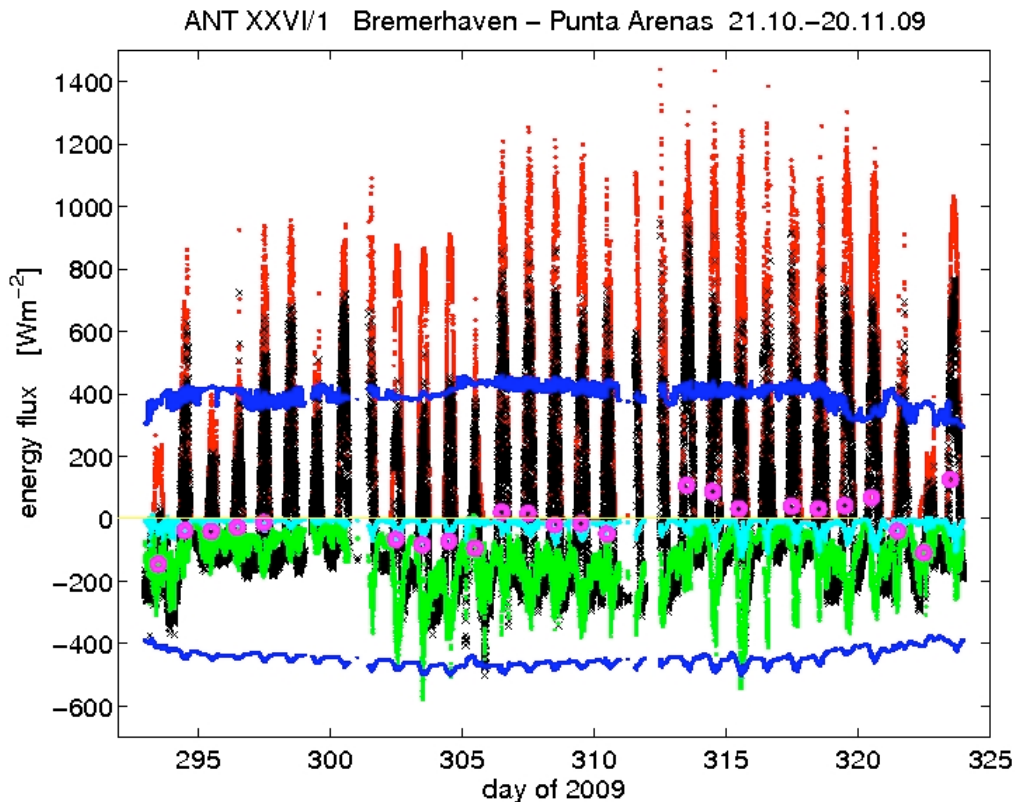


Fig. 3.10: Energy fluxes at the sea surface based in one-minute averages of measurements from OCEANET-Atmosphere: Total balance (black symbols), downwelling longwave radiation (upper blue curve), upwelling thermal radiation (lower blue curve), downwelling solar radiation (red), sensible heat flux (cyan), latent heat flux (green). Daily means have been calculated whenever at least 90 % of the measurements have been available and are denoted by Magenta-coloured symbols. Diagram by Karl Bumke

The lidar measurements show that the marine boundary layer on average reached an altitude of 500 m and that the signal intensity strongly depended on wind velocity. A Saharan dust plume has been observed at 31.10.2009 near the Cape Verde islands. Fig. 3.11 shows the range corrected signal at 1,064 nm at a logarithmic scale with time and position as function of height. *Polarstern* entered the plume at around 01:30 UTC. A nearly aerosol free boundary layer of 500 m height separated the lidar from the dust plume. The top of the plume reached up to 2,500 m height and the base was at around 900 m altitude. From 08:00 UTC until 10:00 UTC shaped structures indicate dynamical processes within the plume. Unfortunately, this time series had to be terminated because of the high sun elevation at 10.25 UTC. Still, we were lucky to obtain a cross section through a Sahara dust layer during our transect.

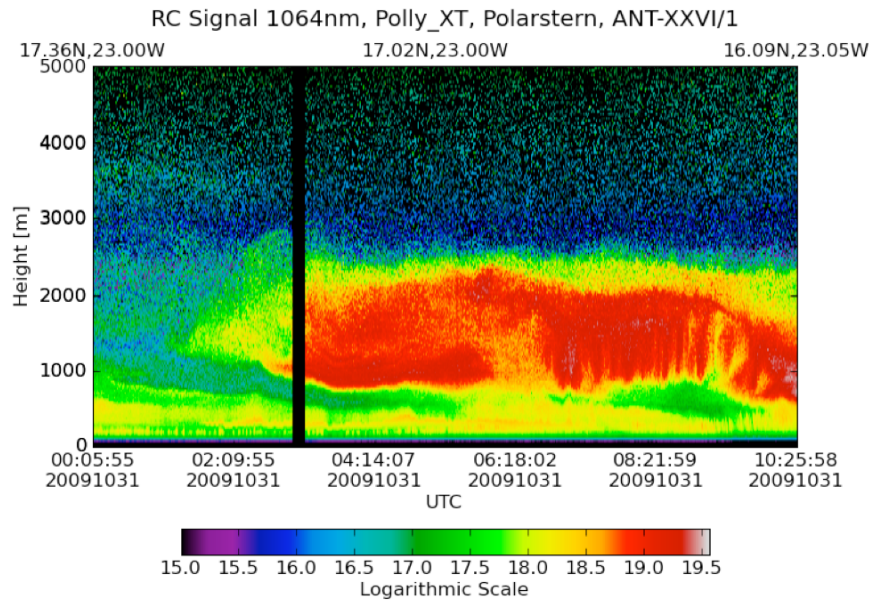


Fig. 3.11: Saharan Dust Plume near to Cape Verde Islands (ANT-XXVI/1, 31.10.2009). Diagram by Thomas Kanitz

Dust has also been observed by Polly^{XT} in the southern hemisphere. Fig. 3.12 shows an aerosol layer at 1.5 km height, which split into two layers at around 01:40 UTC. A strong westerly flow and the analysis of backward trajectories reveal Patagonia as source region.

Fig. 3.12 also impressively shows the large variability of the atmosphere. Both marine boundary layer and aerosol layer moved up and down during night time. Precipitation occurred at about 4,000 m at 21:00 UTC and between 05:00 UTC and 08:00 UTC but did not reach the ground.

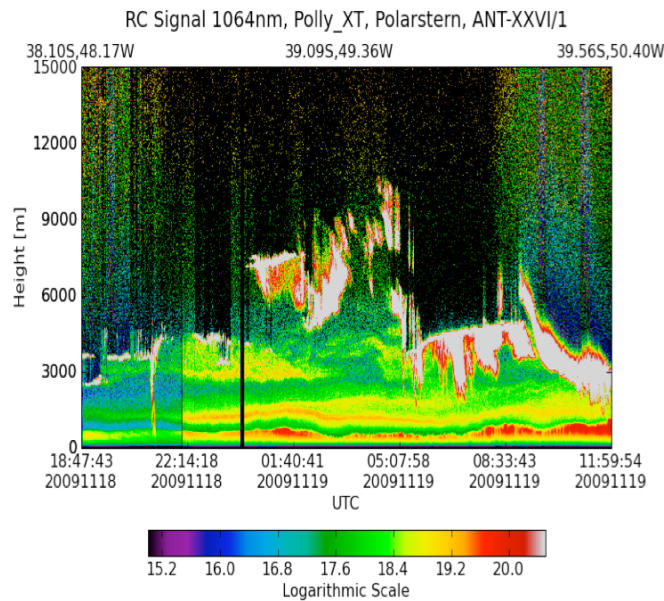


Fig. 3.12: Dust plume from Patagonia (ANT-XXVI/1, 18.11.2009). Diagram by Thomas Kanitz

Overall, the first marine deployment of the Polly-lidar has been very successful. Upon arrival in Punta Arenas the lidar will be parked at a host institute, and will be picked up again for the spring cruise 2010 when *Polarstern* will be heading back to Bremerhaven from its 26th Antarctic expedition.

To check the quality of the data provided by the autonomous meteorological measurement system SCAWS the data have been compared with those of the operational weather station onboard *Polarstern*.

Fig. 3.13 shows the data from one example day from the OCEANET-Atmosphere own meteorological station SCAWS with 1 s temporal resolution and the data provided by the weather station of *Polarstern* with one-minute averages. In general, both systems provide a good correlation, proving that the SCAWS fulfils the specifications that led to its development.

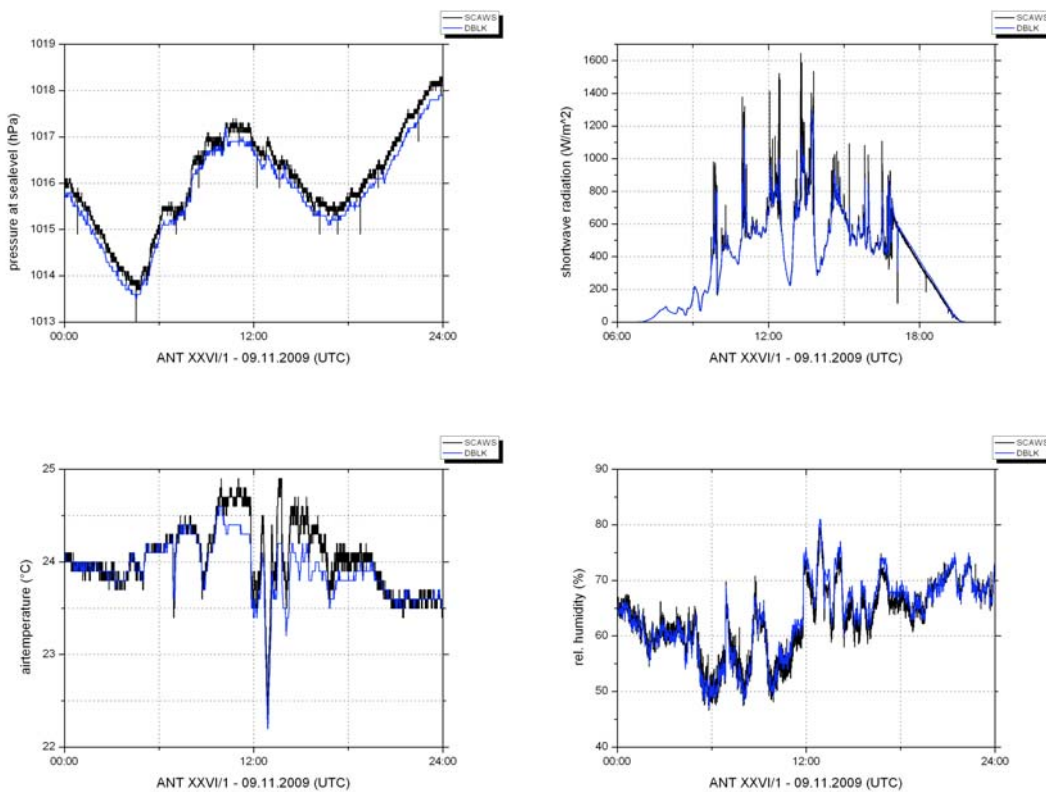


Fig. 3.13: Pressure at sea level, downwelling shortwave radiation, air temperature and relative humidity from the new SCAWS and the *Polarstern* meteorological system. Diagrams by Henry Kleta

The Microtops measurements are part of the Marine AERONET Network, the data of which are available for viewing or downloading on the Aeronet website. It also means that the current results can be directly compared with older *Polarstern* measurements (see Fig. 3.14), or with other research vessels currently in the Atlantic, such as the

RSS *James Cook*, that generally took a more westward course from Great Britain to Punta Arenas (see Fig. 3.15). The figures clearly show that the same Saharan dust outbreak that was recorded by our measurements was also seen by the *James Cook*, but also that in general the atmosphere was relatively pristine during this year.

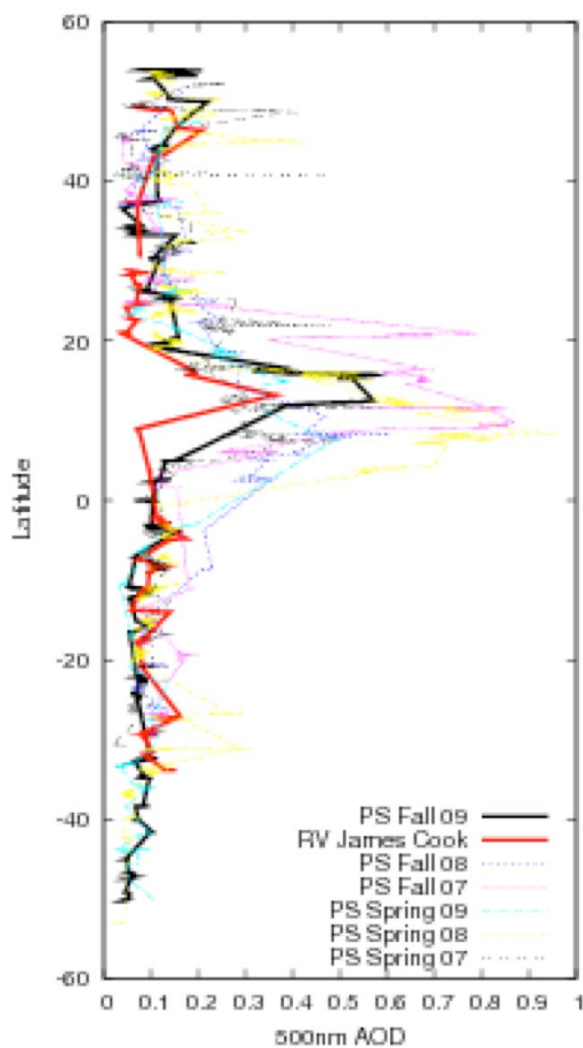


Fig. 3.14: Aerosol optical thickness along cruise tracks of various ship expeditions in the Atlantic. The current expedition of Polarstern is denoted by the thick black line. Diagram by Thijs Heus

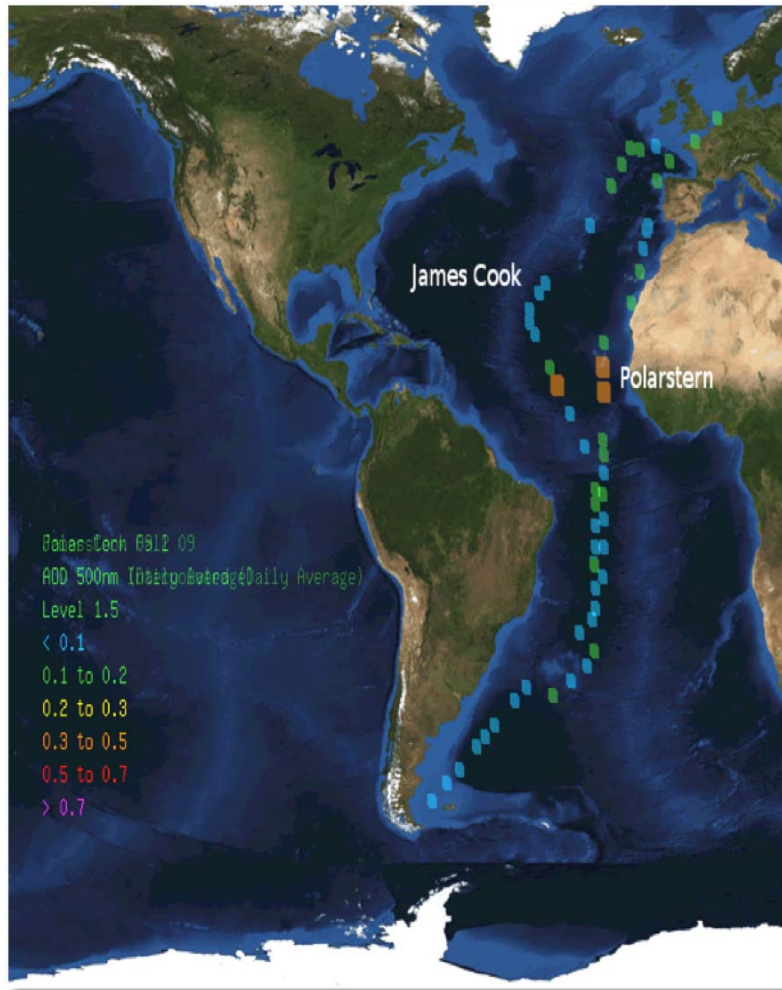


Fig. 3.15: Daily average aerosol optical thickness along the autumn transect cruises of RV James Cook and Polarstern. Diagram by Thijs Heus and AERONET

Finally, within the OCEANET-Atmosphere activities light regimes in the ocean are observed.

The light variability in the upper layer strongly depends on surface elevation and thus sea state conditions. The first meters (< 5 m) show quick and intense variations in light intensity due to the focusing-defocusing effect of the surface waves. At larger depths fluctuations attenuate in frequency and amplitude. The RAMSES radiometer data show extreme peaks in the downwelling irradiance above 10 m, which occasionally exceed the values at above sea level. With increasing depth the mean intensity decreases exponentially.

Fig. 3.16 shows a typical depth profile of downwelling irradiance at a wavelength of 495 nm (bluish light) and mean intensity values per depth. The red line indicates the irradiance at the surface at that wavelength.

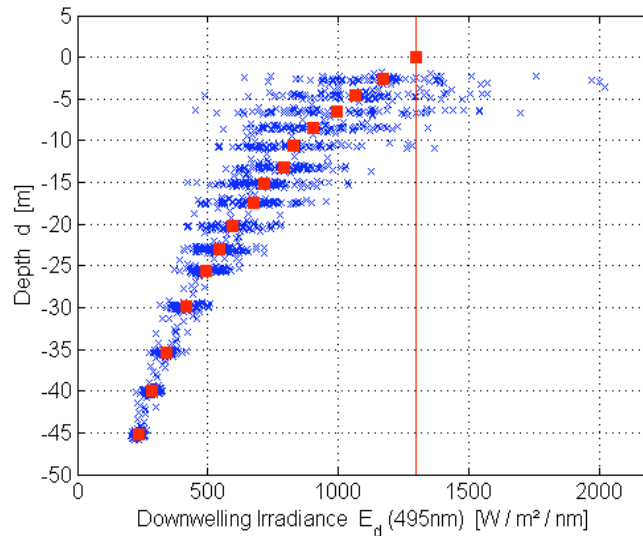


Fig. 3.16: Downwelling irradiance at wavelength 495 nm in the upper layer (ANT-XXVI/1, 30.10.2009). Diagram by Martin Hieronymi

By means of the underwater camera system spatio-temporal light fields can be quantified and radiometer data can be interpreted in a better way. Fig. 3.17 shows sample pictures of four depths and time development of a pixel’s brightness at the particular depths. Dominant periods and standard deviations of the time signals are highlighted.

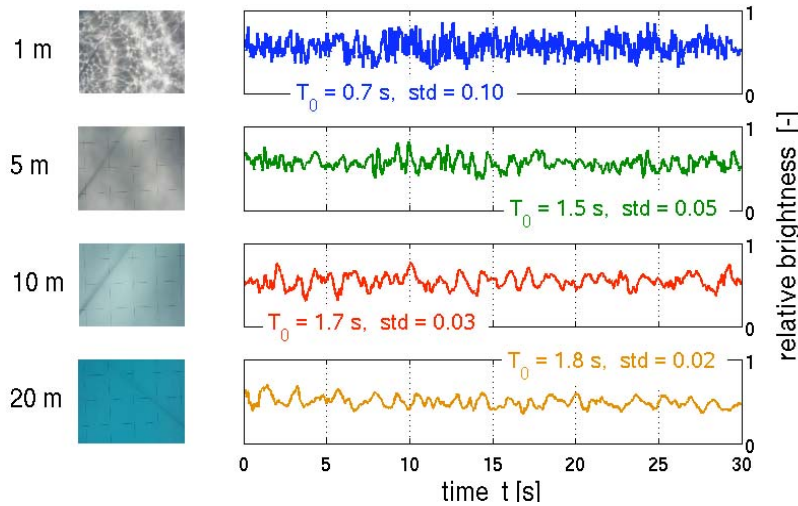


Fig. 3.17: Left: Example pictures from underwater camera device at different depths, right: time series of one pixel’s brightness at corresponding depths. Diagram by Martin Hieronymi

One aim of these measurements is to obtain realistic training datasets for radiative transfer simulations under diverse sea state conditions. Another purpose is the validation of satellite based ocean colour retrievals, done in cooperation with the Phytooptics group at AWI and University Bremen.

4. ABYSSAL TEMPERATURE FLUCTUATIONS IN THE VEMA CHANNEL

Hannah Weber¹, ¹IFM-GEOMAR, Kiel
not on board: Walter Zenk¹, Martin Visbeck¹

Objectives

The equator bound flow of Antarctic Bottom Water (AABW) represents a significant limb of the global thermohaline circulation. In the South Atlantic the deep western boundary along the continental rise carries AABW northward. The advected water masses originate from the Weddell Sea, where they are formed by deep winter-time convection. At the latitude 32°S the abyssal flow encounters two topographical constrains in form of the zonally aligned Santos Plateau and the Rio Grande Rise. These combined submarine mountain chains separate the Argentine Basin in the south from the Brazil Basin farther to the north. AABW finds its equatorward pathway through this natural impedance via a 790 km long canyon called Vema Channel (Fig. 4.1). The meridionally directed channel with water depths > 4,500 meters provides a choke point for observations of water mass property and transport fluctuations of abyssal waters. Monitoring such fluctuations is vital for a state-of-the-art modelling of the global climate system.

A decade-scale record from the channel entrance (31°S 39°W) indicates a clear increase of the lowest temperatures of the bottom water. Comparable observations from the exit region of the Vema Channel (26°S 34°W) confirm the general abyssal temperature rise since 1991. The Vema Sill station at the entrance is internationally acknowledged as an ocean site observatory. *OceanSITES* is a worldwide system of long-term, deep water reference stations measuring regularly dozens of physical, geochemical, and biological variables (<http://www.oceansites.org>).

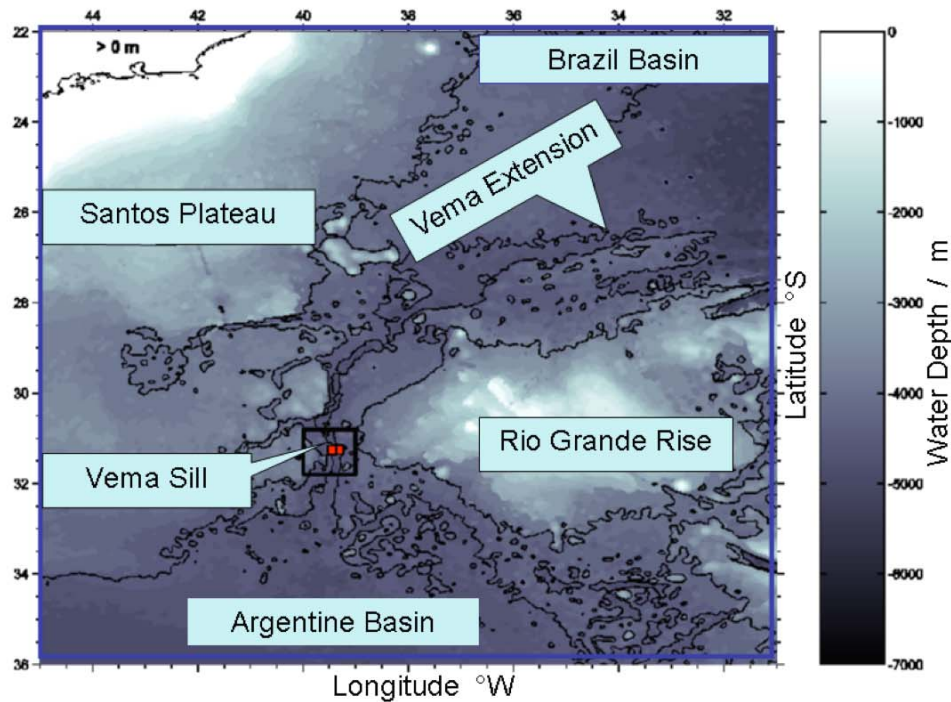


Fig. 4.1: Vema Channel in the South Atlantic. This canyon enables dense Antarctic Bottom Water to leave the Argentine Basin on its equator bound drift towards the Brazil Basin. Revisits to the Vema Extension and the Vema Sill were successfully accomplished during ANT-XXVI/1.

Work at sea

Our prime objectives during ANT-XXVI/1 were revisits to the Vema extension and sill sites for additional high precision CTD observations of the coldest AABW in the Vema Channel (see Fig. 4.1). On both stations temperature and salinity profiles down to 8 meters above the ground were obtained (Stations nos. 25 and 25).

Preliminary results

While repeat visits at the sill site near the channel entrance started already in 1972, the first dedicated CTD station at the exit of the Vema Channel was obtained in the beginning of the World Ocean Experiment (WOCE) in 1992. Table 4.1 shows the available collection of CTD stations. On eight revisits to the Vema extension the series of lowest potential temperature of bottom water could be extended.

Tab. 4.1: Compilation of CTD stations and measured potential temperature minima with pertinent salinity values from the Vema Extension. For position of this site see Fig. 4.1.

Visit Nr.	Ship/ Cruise/ Expedition	Date	Lat.° S	Lon.° W	Pot.Temp .° C	Salinity @min. Pot. Temp.
1	Meteor/22/leg 4	1992-12-18	26.89	34.79	-0.133	34.676
2	Meteor/34/leg 3	1996-03-11	26.87	34.80	-0.112	34.670
3	Meteor/41/leg 3	1998-04-23	26.70	34.23	-0.099	34.674
4	Ak. S. Vavilov/17/leg 1	2003-11-03	26.72	34.20	-0.095	34.675
5	RSS Discovery/276	2003-12-15	26.60	33.70	-0.081	34.676
6	Polarstern/ANT- 22/5	2005-06-02	26.70	34.23	-0.081	34.673
7	Polarstern/ANT- 25/5	2009-04-26	26.70	34.23	-0.079	34.672
8	Ak. Ioff/90	2009-04-18	26.72	34.20	-0.067	34.676
9	Polarstern/ANT- 26/1	2009-11-14	26.68	34.22	-0.075	34.674

Fig. 4.2 displays the series of potential temperature/salinity since 1992. All numbers (E1-E9) correspond to the nomenclature in Zenk and Morozow (2007). The last dot is labelled by an extra star in the centre. Note that this ANT-XXVI/1 observation is the first one in the row from the Vema Extension which shows a light reduction of the measured lowest potential temperature. In all other cases a systematic temperature rise has been observed since 1992. Actual numbers are given in Table 4.1.

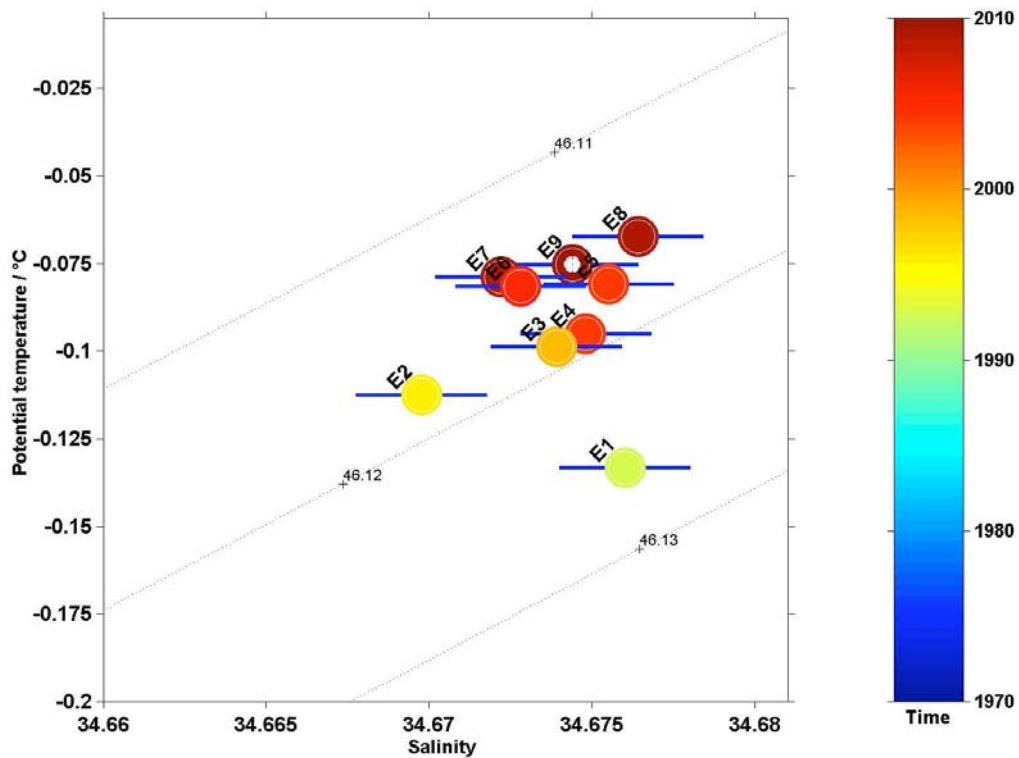


Fig. 4.2: Evolution of potential temperature and associated salinity data from the Vema Extension with isopycnals referenced to 4,000 dbar (σ_θ in kg m^{-3}). For details see also Table 4.1. The horizontal bar indicates salinity estimated measurement errors. The centred white star depicts the last observation, i.e. from ANT-XXVI/1. Note the almost continuous temperature rise, since E1 values was obtained.

Reference

Zenk, W., E. Morozov (2007), Decadal warming of the coldest Antarctic Bottom Water flowing through the Vema Channel, *Geophys. Res. Letters*, 34, L14607, doi:10.1029/2007/GLR030340.

5. TEST OF A 25.1 MM UMBILICAL CABLE INSTALLED ON THE MOBILE *METEOR* FRICTION WINCH ON BOARD OF *POLARSTERN*

Reinhard Werner¹, Thomas
Ohms², Sonja Löffler³, Klaus
Müller⁴, Andreas Pluder⁵,
Andreas Rex⁶, Johannes
Rogenhagen⁷, Andreas
Schrapel⁶

¹IFM-GEOMAR, Kiel

²Control Station Meteor / Merian, Hamburg

³DFG-Senatskommission für Ozeanographie,
Bremerhaven

⁴Hatlapa Uetersener Maschinenfabrik GmbH & Co
KG, Uetersen

⁵Reederei F. Laeisz (Bremerhaven) GmbH

⁶RF Reederei Forschungsschiffahrt GmbH,
Bremen

⁷Fielax GmbH/ Reederei F. Laeisz (Bremerhaven)
GmbH

Objectives

The mobile Meteor friction winch (manufacturer Hatlapa Marine Systems) consists of a storage winch (20 kN) and a friction winch (150 kN) and belongs to the „Meteor large equipment pool“. Both units have 20´container dimensions and weight approximately 20 t (incl. cable) and 18t, respectively. The storage winch is equipped with a 3.500 m long 25.1 mm umbilical cable manufactured by JDR Cable Systems. The winch and the cable have been designed to deploy heavy instruments with high electrical power requirements such as, for example, the Rockdrill II by the British Geological Survey (BGS) in water depths up to 3,000 m. Rockdrill II is the latest generation of remotely operated sub-sea rockdrills. This new rockdrill can continuously core in 1.5 m sections up to a total of 15 m below seabed in water depths of 3,000 m or 10 individual cores, each up to 1.5 m, in a localized area. Because of its power requirements and weight, Rockdrill II cannot be operated with the cables usually installed on the winches of research vessels. The next deployment of the mobile Hatlapa winch with Rockdrill II is scheduled for summer 2010 onboard R/V *Sonne* in the framework of the research project SO-208 PLUMEFLUX (15.07.2010 - 29.08.2010). SO-208 is a project of the working group of Prof. Hoernle (RD 4, IFM-GEOMAR) and aims at systematic sampling of the Galápagos Spreading Center (East Pacific) by drilling across ridge profiles in water depths of 2,000 – 3,000 m. During its last deployment in deep water conditions on R/V *Meteor* in 2007, however, the outer armour of the JDR umbilical started to unwrap while deploying Rockdrill II. Accordingly the mobile *Meteor* friction winch was not serviceable with the JDR umbilical cable in its condition at that time. Three possible reasons have been considered which may have caused this problem:

- (1) The JDR umbilical cable already had problems on delivery.
- (2) The JDR umbilical cable got twisted during deployment.
- (3) The unfavourable arrangement of the friction winch and the storage winch on the deck of R/V *Meteor* caused the problem. *Meteor's* working deck proved to be too small to arrange the storage winch and the friction winch properly in a row on the same level. Instead the storage winch was installed on the hatchway, i.e. higher than the friction winch. This arrangement made it necessary to fix the pulley which leads the cable from the storage winch to the friction winch. Otherwise the umbilical cable would have been in contact with the frame of the friction winch.

Therefore we proposed to carry out a test programme on *Polarstern* cruise ANT-XXVI/1 to identify the reasons of the problems with the cable and - ideally – to restore the operability of the winch with the JDR umbilical cable. *Polarstern's* deck allows a proper arrangement of friction and storage winches (on the same level) and the vessel operates on ANT-XXVI/1 in areas with more than 3,000 m water depth where a complete extension of the umbilical cable is possible. Restoring the operability of the mobile *Meteor* friction winch with the JDR cable is a major prerequisite for its future use and the gained knowledge on how to solve such problems is invaluable if they should appear again.

Methods/work at sea

The test programme was conducted at three positions in the area between 38°N and 36°N west of Portugal. We carried out the following sequence of test:

- 1) Wire lowered with a weight of 200 kg at a speed of 1.0 m/sec to 3,150 m (max. depth). Hoisting on deck with a speed of app. 0.3 to 0.4 m/sec*.
- 2) Lowering with a weight of 200 kg at a speed of 1.0 m/sec to a depth of 1,000 m. Hoisting with 1.0 m/sec on deck.
- 3) Cable lowered with a weight of 5,000 kg at a speed of 1.0 m/sec to depths of 700 m, 1,500 m, 2,000 m, 2,500 m (short heave test at each position). Cable brought down to sea floor at 2,608 m water depth and 2,650 m cable length. By putting the weight on the sea floor the operation of Rockdrill II has been simulated. Cable and weight hoisted at a speed of 0.5 – 0.8 m/sec* on deck.
- 4) Cable lowered with a weight of 5,000 kg at a speed of 1.0 m/sec to depths of 700 m, 1,500 m, 2,000 m (short heave test at each position). Cable and weight hoisted at a speed of 1.0 m/sec up to 700 m.
- 5) At 700 m depth cable and weight have been hoisted shortly with a speed of 1.0 m/sec. Subsequently cable and weight were lowered at 1.0 m/sec to 1,500 m and hoisted on deck with the same speed.

* The low hoisting speed during test (1) and (3) was caused by too high a current consumption under load. This malfunction was caused by wrongly adjusted set points of electrical components. The fault was rectified.

Results

The observations made in course of the tests are:

- The cable had never been lowered by more than app. 620 m before this test.
- The cable is damaged on the first 620 m, meaning that the outer armour is turned open in certain, local areas. Especially at ~605 m the outer armour is detached from the inner one and gaps have formed. Additionally the cable is deformed (wave – like pattern) up to a length of ~620 m. However none of the single strands in the armour is broken. It is assumed that those damages had been caused by the method of cable installation on the friction winch previously used. Because of the installed termination the cable had to be put on in slings.
- From ~620 m on the cable is in factory - delivery – condition.
- During the test **no** twisting and opening of the armour has been observed. Inside the friction the cable is neither compressed nor pushed. The cable reels in and out in a satisfactory manner. Except for the already known damages on the first 620 m nothing conspicuous was noted.

In conclusion, the JDR umbilical cable installed on the mobile Meteor friction winch is ready for service between 620 m and 3,500 m. The operation of the first 620 m is risky and has to be avoided.

This problem can be solved by turning the JDR cable so that the damaged 620 m will remain on the drum of the storage winch. We consider that as best solution because after turning the cable can be deployed from the mobile Meteor friction winch without any restrictions up to a depth of 2,900 m. Prior to the turning the cable has to be thoroughly tested (Coax, power supply, optical fibre). If turning of the cable proves impossible for any reasons, the cable will be cut at ~620 m. In this case the cable can be deployed up to a depth of 2,600 m only.

Cutting or, preferably, turning of the JDR cable would restore the operability of the mobile Meteor friction winch with that cable in water depths up to 2,600 and 2,900 m, respectively. It would allow to carry out the research project SO-208 PLUMEFLUX without significant restrictions. However, apart from turning the cable and testing/measuring optical fibre, Coax, power supply, several requirements must be fulfilled before the cable can be used with the Meteor friction winch on board RV *Sonne*. These include modification of the termination of the cable and of the winding-off sheave on the friction winch as well as complete service of the winch by the manufacturer. Furthermore the weights of both winch containers have to be verified.

6. AUTONOMOUS MEASUREMENT PLATFORMS FOR SURFACE OCEAN BIOGEOCHEMISTRY (OCEANET): OCEAN

Steffen Aßman^{1/2}, Peer Fietzek¹, Martina Gehrung²,
not on board: Arne Körtzinger¹, T. Steinhoff¹, J. Bock³, G. Friedrichs³, M. Hoppema⁴, S. van Heuven⁵, H. Zemmeling⁵, F. Schröder², W. Petersen²

¹ IFM-GEOMAR
² GKSS
³ CAU Kiel
⁴ Alfred-Wegener-Institut, Bremerhaven
⁵ NIOZ

Objectives

The aim of the WGL-PAKT-Initiative OCEANET is to develop new autonomous instruments for the investigation of energy and matter exchange at the air-sea interface. The multi-institutional participants from IFM-GEOMAR, GKSS, IfT and AWI intend to build up a sensor network that investigates atmospheric and surface ocean properties. In order to meet the growing demand for increased spatial and temporal data, autonomous sensor networks that can be deployed on merchant vessels are needed. Tests of new instruments and measuring techniques as well as the installation of instrumentation aboard *Polarstern* are essential components of the project.

The oceanic component of this study focuses on the marine carbon cycle in the surface ocean which is of high climate relevance but at the same time susceptible to climate change. The surface ocean's CO₂ source/sink function is maintained by a complex interaction of physical and biological processes. Therefore its understanding requires measurement of various different parameters as it is pursued within OCEANET.

The work carried out during earlier transit expeditions (ANT-XXIV/4, ANT-XXV/1 and 4) will be continued. During the first OCEANET cruise the feasibility of autonomous underway measurements was assessed for a wide range of instruments for measurement of physical (temperature, salinity, turbidity), chemical (CO₂ partial pressure ($p\text{CO}_2$), pH, oxygen, total gas tension, nutrients), and biological parameters (chlorophyll a, photosynthetic parameters) and small intercomparison for measurements of $p\text{CO}_2$ took place. Within the second cruise the focus was on intercomparison measurements of CO₂ partial pressure with diverse autonomous underway flow-through as well as submersible systems. The work on the third transit dealt with the closer investigation of a commercial submersible $p\text{CO}_2$ -sensor and included CTD cast with the instrument. Underway $p\text{CO}_2$ -measurements were run as a reference. Nitrate and nutrient determinations were part of the work as well.

During ANT-XXVI/1 an optimized and improved submersible $p\text{CO}_2$ -sensor was investigated in detail. The instrument's data will be intercompared with data obtained by the underway system installed on *Polarstern*. The different biogeochemical regions crossed during the cruise and its duration provided good conditions for comprehensive testing of instrumentation.

For the first time a cavity ringdown spectrometer (CRDS) was successfully used for the determination of the $\delta^{13}\text{CO}_2$ isotopic ratio of surface water within an underway setup. In addition to the isotopic ratio the instrument provided a $p\text{CO}_2$ dataset, which will be included in the intercomparison. Additional data for dissolved oxygen (O_2) concentration and total gas tension were measured as additional and relevant chemical parameters for the executed investigations. Furthermore, experiments with a newly developed optical pH-sensor were conducted. Carbonate system investigations would benefit from progress in this field.

Since this expedition a comprehensive underway-system, a so called "FerryBox", is permanently installed on *Polarstern* providing physical, chemical and biological data. Already on two transects, ANT-XXIV/4 and ANT-XXV/4, a transportable FerryBox was had been in use. This system runs automatically and is to be supported by the crew to start and stop of the measurements.

Work at sea

Flow-through box

Three different submersible sensors were used in an underway setup during this cruise: one for the measurement of $p\text{CO}_2$, one for O_2 and one for the measurement of the total gas tension (see Fig. 6.1). They were placed in a thermally insulated flow-through box with a volume of about 80 L. The box was continuously flushed with water from the ship's seawater supply with about 16 L/min, drawn from around 11 m depth via a centrifugal pump and delivered via stainless steel tubings. This principle had proven its functionality during previous cruises. Temperature and salinity necessary for the later analysis were measured directly at the seawater intake by the shipborne thermosalinograph.

The $p\text{CO}_2$ sensor under investigation was a HydroC™/CO₂ (CONTROS Systems and Solutions GmbH, Kiel, Germany). Within this sensor of cylindrical shape a flat silicone membrane acts as an equilibrator between the seawater and the inner gas volume of the sensor. The CO_2 concentration in the internal air circuit is measured by means of NDIR detection. The HydroC™ was successfully used within the flow-through box throughout the entire cruise.

For the measurement of O_2 an oxygen optode sensor (Aanderaa, Bergen, Norway) was used. It measures the *in-situ* water temperature along with the dissolved O_2 concentration and can therefore be used to account for the effect of warming of the sample flow between intake and point of measurement. The optode ran throughout the whole cruise without any interference.

The third sensor in the box was a gas tension device (HGTD, Pro Oceanus, Halifax, Canada). It measures the total pressure of all dissolved gases in the seawater. This important parameter for the measurement of dissolved gases will be included in the analysis of the other sensors' data. Its measuring principle is based on membrane equilibration between the water and an internal headspace in which a pressure sensor is installed. The tube shaped membrane needs a separate continuous stream of water in order to provide a reasonable response time and reproducible equilibrations properties. A submersible pump is therefore connected to the HGTD. Unfortunately two pumps broke during the cruise so that the gas tension dataset does not cover the complete transect.

Flow Through Systems

The dataset obtained with a GO/Neill underway $p\text{CO}_2$ measurement system (General Oceanics Inc., Miami, Florida, USA), which is permanently installed on *Polarstern*, will be used as a reference system for the HydroC™ and the cavity ring-down spectrometer setup described below, since it is the most intensively tested and internationally accepted system for $p\text{CO}_2$ measurements. Before putting the system into operation some maintenance work was carried out, which became necessary due to unusual observations in the $x\text{H}_2\text{O}$ signal of the installed NDIR CO_2 detector (LiCOR 7000). New Nafion®-tubes were installed, a drying cartridge was built in and the NDIR detector was replaced by an identical unit for the time of the cruise. Beside some short interruptions the GO-dataset covers the entire cruise.



Fig. 6.1: Picture of the in-situ sensors inside the flow-through box (from left to right): HGTD sensor with a connected pump (blue), HydroC™/CO₂ and oxygen optode.

A second GO/Neill underway $p\text{CO}_2$ measurement system was set up in a slightly modified variant and used for the first time on sea together with a new detector type: a cavity ringdown spectrometer (CRDS; EnviroSense 2050, Picarro Inc.). Beside the measurement of $p\text{CO}_2$ this optical instrument determines the isotope resolved concentrations of $^{12}\text{CO}_2$ and $^{13}\text{CO}_2$. The isotope ratio is another significant parameter for the investigation of the carbon cycle. The system measured successfully throughout the entire cruise without any interference. Its $p\text{CO}_2$ data will be included into the intercomparison of the other sensors' data.

For a comprehensive specification of the CO_2 -system an accurate determination of the pH value is a necessary task. It was realized during this trip by means of a newly developed optical pH-sensor. The measuring principle comprises a spectrophotometric pH determination based on the absorbance spectra of a pH sensitive indicator dye. As a light source a broadband white LED is used. Entire absorption spectra (430 - 700 nm) are recorded and used to precisely calculate the

pH. In order to improve the accuracy of the sensor, different experiments were carried out during this transect. The temperature stabilization was modified, different possibilities of guiding the light into the optical system were tested and the measuring routine was improved.

Within the framework of OCEANET a FerryBox had been permanently installed on *Polarstern* since this expedition. It is connected to the same seawater supply as all the other systems described above. The FerryBox (4H-Jena Engineering GmbH) is a position-controlled, low maintenance measuring system, which was designed for autonomous, long-term application on ships or other measuring platforms to enable a basic, but nevertheless extensive description of the water condition. Therefore oceanographic, chemical and biological parameters such as temperature, turbidity, salinity, pH, oxygen, chlorophyll a, phycocyanin and CDOM are measured. Not all of the sensors were calibrated. The FerryBox worked reliably throughout the complete transect.

The installation of the FerryBox was carried out before the stop in Las Palmas. The following actions were taken:

1. Adjust the water flow from the ship internal seawater system to the process control of the FerryBox.
2. Install a bypass system with a cross-flow filter. The discrete optical pH-measurements use this to get seawater without particles or organic substance.
3. Test the automatic data transfer per email.
4. Check and installation of the calibrate files of the sensors.
5. Test measurements were carried out.
6. Training the crew to handle the FerryBox.



Fig. 6.2: FerryBox

Sampling and CTD casts

As a point based reference for the tested $p\text{CO}_2$ systems and for the total description of the carbonate system discrete samples for dissolved inorganic carbon (DIC) and total alkalinity (TA) were taken for analysis back home at the IFM-GEOMAR in Kiel. The samples were drawn into 500 mL bottles and poisoned with saturated mercuric chloride solution.

A second HydroC™/CO₂ was used during CTD experiments to allow for the analysis of the depth dependent response and overall behaviour of the sensor at water depth of up to 2000 m. The sensor and its configuration were optimized after every cast. Depth water samples were taken as reference as well.

Preliminary and expected results

High-quality data in a high temporal resolution along the meridional surface transect through the Atlantic Ocean was collected. Especially in the South Atlantic regions starting at 33°S we observed heavy bloom events as well as strong temperature and salinity gradients. These provided perfect testing conditions for the instruments, which all proved their functionality. The FerryBox provided plots in real-time of various parameters and thus successfully helped identifying these events (see Fig. 6.3).

The combined data set of autonomously recorded and discrete samples will provide a detailed insight in the carbon chemistry of the surface waters including isotope dependencies. An intercomparison between different $p\text{CO}_2$ instruments (HydroC™/CO₂, GO-system, CRDS) will be carried out. The fact that all parameters of the carbonate system were measured (pH, $p\text{CO}_2$) or sampled for (DIC, TA) allows for the comparison of one parameter's dataset with a dataset derived from the other measured quantities.

The following datasets were collected and their evaluation as well as analysis is underway within the respective institutions:

- Autonomous continuous measurements of $p\text{CO}_2$ in surface waters with different instruments:
 - HydroC™/CO₂ (submersible) – IFM-GEOMAR
 - GO/Neill-system (underway) – NIOZ, IFM-GEOMAR, AWI
 - CRDS (underway) – CAU Kiel, IFM-GEOMAR
- Autonomous continuous measurements of dissolved oxygen and total gas tension (until November 11) in surface waters – IFM-GEOMAR
- Autonomous continuous measurements of $\delta_{13}\text{CO}_2$ in surface waters (CRDS) – CAU, IFM-GEOMAR
- Autonomous discrete optical pH-measurements – IFM-GEOMAR, GKSS
- Autonomous continuous measurements of temperature, turbidity, salinity, pH, oxygen, chlorophyll a, phycocyanin and CDOM (FerryBox) – GKSS
- Dissolved inorganic carbon and alkalinity will be derived from water samples taken every 8 hours – IFM-GEOMAR
- *In-situ* $p\text{CO}_2$ measurements on the CTD (up to 2,000 m; HydroC™/CO₂) – IFM-GEOMAR

The intercomparison of different $p\text{CO}_2$ systems as well as the optimization of the HydroC™ and the pH sensor are ongoing tasks and will be continued during the next cruises with OCEANET participation (ANT-XXVI/4).

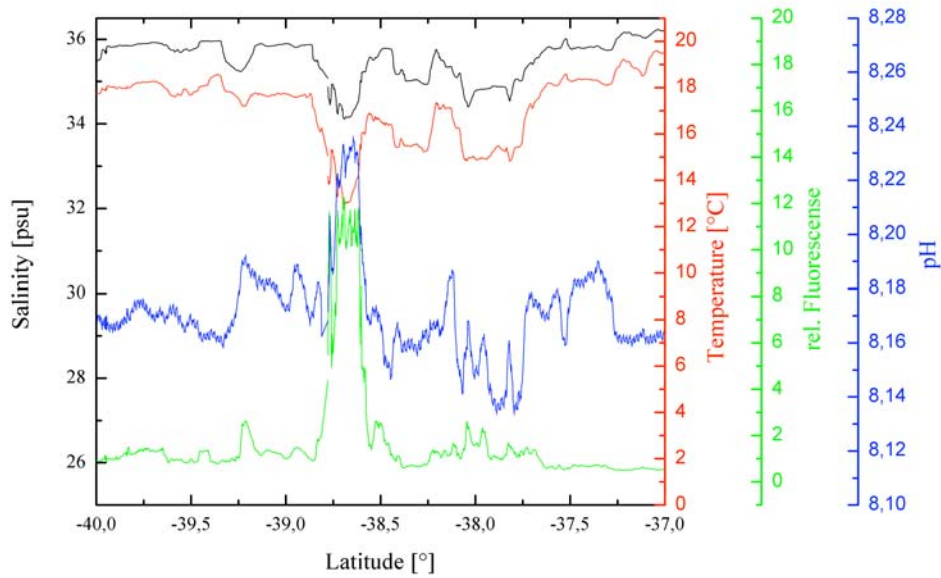


Fig. 6.3: Parameters measured by the FerryBox indicating a strong bloom event at around 39°S in the Southern Atlantic.

7. SEA TRIAL AND TESTS OF THE FIBRE OPTICAL 18 MM CABLE (LWL) AND THE TELEMETRY SYSTEM

Saad El Naggar¹, Andreas Pluder²,
Johannes Rogenhagen², Thomas Feiertag²,
Heiko Liellenthal³

¹ Alfred-Wegener-Institut,
Bremerhaven
² F. Laeisz
³ SITEC

A new 18 mm fibre optical coax cable (8,000 m) had been purchased and it was planned to be installed on board *Polarstern* during the last shipyard stay in Bremerhaven between 25 Sept and 16 Oct 2009 providing state-of-the-art of communications to scientists.

New designed telemetry system was also developed and installed to provide to the multiuser a common platform for power supply and underwater data communications.

The sea trial and tests of the system under real operation conditions were planned to be carried out during the cruise ANT-XXVI/1 on the way between Bremerhaven and Las Palmas (16 – 27 Oct 2009).

Unfortunately the planned trial programme had to be completely cancelled due to a delay in delivering the cable.

A coax cable-based telemetric system was successfully tested instead during this cruise (see chapter 12) to provide a wide range of users online high quality video images via standard coax cable to control marine instruments operated at seafloor. This system is now operational and available on board for all users.

8. SEA TRIAL AND TESTS OF THE UPGRADED UNDER WATER NAVIGATION SYSTEM “POSIDONIA”

Saad El Naggar¹, Gerd Rohardt¹,
Johannes Rogenhagen², Werner Dimmler²

¹ Alfred-Wegener-Institut,
Bremerhaven
² F. Laeisz

Objectives

The underwater navigation system POSIDONIA had been upgraded during the ship yard stay of *Polarstern* in Bremerhaven between 20 May and 12 Jun 2008.

Newly designed hard and software were installed and tested at the harbour in Bremerhaven.

The new acoustic array and window were fix-installed nearby the moon pool in addition to the mobile acoustic array.

A complete new electronic cabinet was installed, modified and tested.

The first operational test under real conditions at sea had been carried out during the cruise ARK-XXIII/1+2.

A final sea trial and calibration were planned to be carried out during the cruise ANT-XXV/1 on the way to Las Palmas during the time between 03 Nov and 10 Nov 2008 at a water depth of more than 3,000 m.

The planned calibration and sea trials were not carried out during ANT-XXV/1 due to the technical problems occurred to the system. The system was faulty and not operational.

During the last shipyard stay in Bremerhaven, 24 May to 20 Jun 2009, the damaged acoustic array and window were repaired by replacing new components.

The system was successfully used during ARK-XXIV cruise, but the new acoustic array was not operable due to the diffraction occurred by the protection window. The system was not able to locate the target exactly and within the expected error bias.

During ANT-XXVI/1 and on the way between Bremerhaven and Las Palmas (16– 27 Oct 2009) the system was tested and calibrated.

Work at sea

- Complete and tune the final installation according to the claims found out during the first sea trial tests on ARK-XXIV/1+2
- Mooring of calibration transponder
- Sea trial, calibration and acceptance tests at location (about 24 hours)
- Recovering of the transponder
- Data analysis and validations
- Real operations between test location and Las Palmas
- Disembarking the test team in Las Palmas on 27 Oct 2009.

General conditions during the calibration and tests:

Date: 23 Oct 2009
Transponder Position: 36°3.45' N; 12° 59.23' W
Transponder depth: 2,515 m
Water temperature: 21.8°C
Air temperature: 21.8°C
Sea state: 3 m swell
Wind speed: 4.5 m/s
Wind direction: 233°

Track circle diameter: about 1,800 m
Ship speed during measurement: 3 knots
All other acoustic systems are OFF

Start of tests: 23 Oct 2009; 07:55 UTC
End of tests: 24 Oct 2009; 07:23 UTC

Mooring configuration (Fig. 8.1):

Two transponders (RT861 B1S; Nr. 566 and 567)

First trial and data set:

Used acoustic array: Fixed array with protection window
Used POSIDONIA system: New system POSIDONIA 6000

First data analysis: Calibration was not possible due to the multipass (diffraction), which maybe occurred by the protection window (see Fig. 8.2).

Second data set:

Used acoustic array: Fixed array with protection window
Used POSIDONIA system: Old POSIDONIA system VME

First data analysis: Calibration was not possible, due to the multipass (diffraction) which maybe occurred by the protection window, like the first data set (see Fig. 8.3).

Third data set:

Used acoustic array:	Mobile array, moon pool installation
Used POSIDONIA system:	New POSIDONIA system 6000

First data analysis: Calibration was successful. Accuracy about ± 12 m (see Fig.8.4)

Calibration parameter set:	Heading:	- 0.61°
	Roll:	+0.17°
	Pitch:	- 0.04°

Conclusion

The new acoustic fixed array is not fully operational and it was not possible to have it calibrated. The protection window causes a lot of disturbance in a correct positioning of transponder. Further investigations will have to be done to improve the acoustical characteristic of the fixed array.

The mobile array is still operational and could be immediately used.

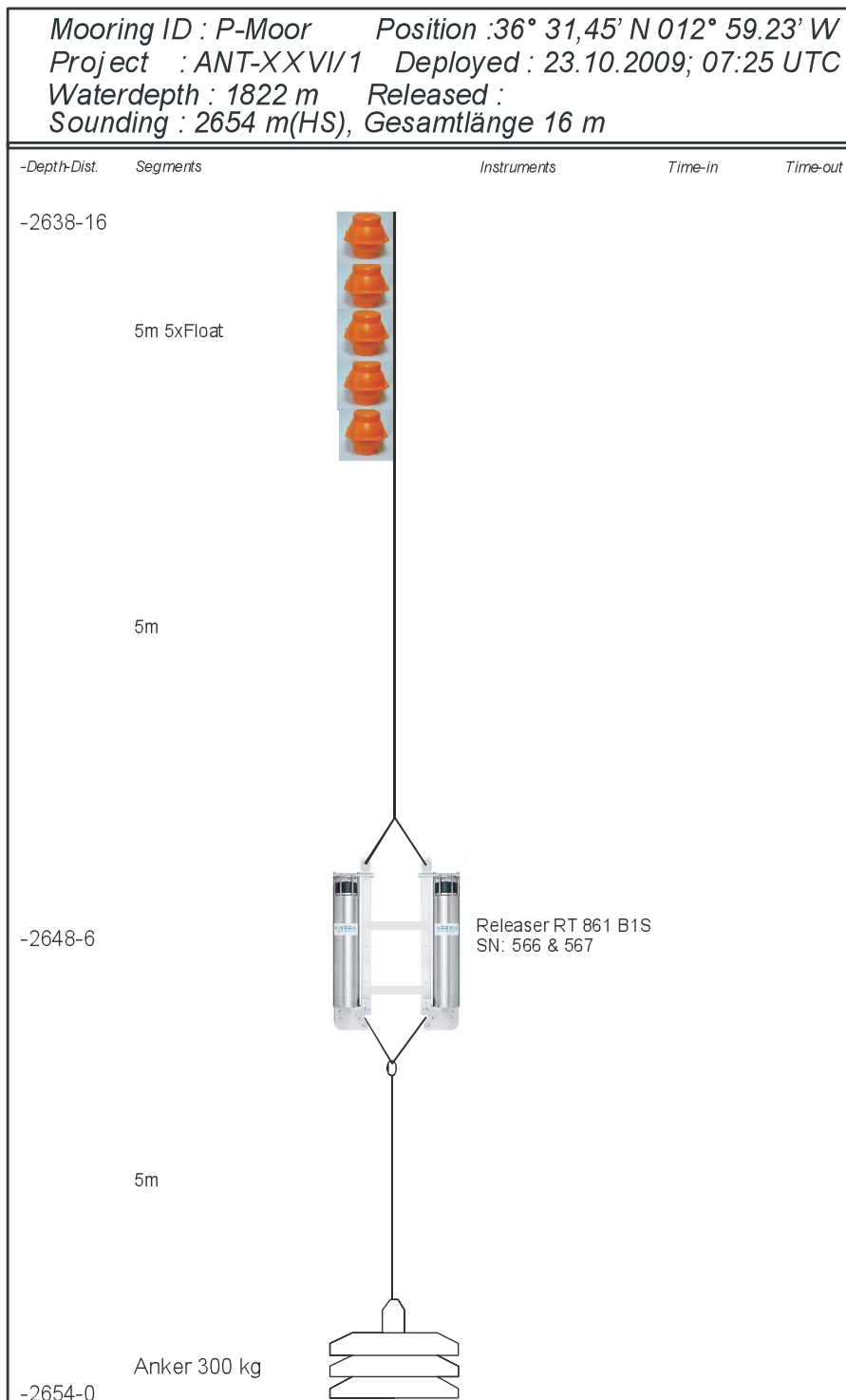


Fig. 8.1: Mooring configuration

8. Sea trial and tests of the upgraded under water navigation system "POSIDONIA"

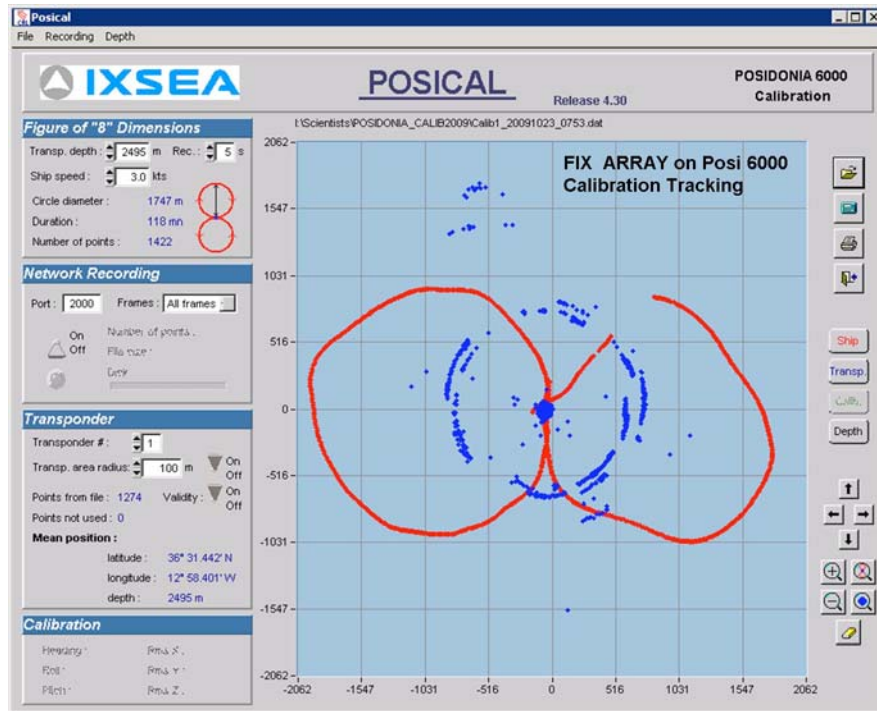


Fig. 8.2: Calibration of the fixed acoustic array. Red line = Ship's track, Blue dots = Detected transponder positions

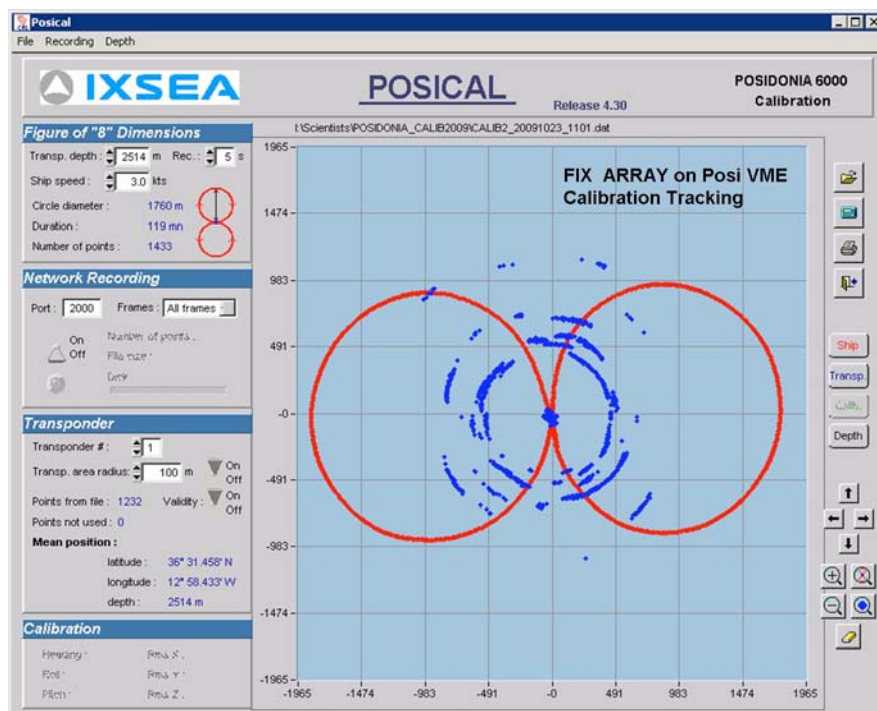


Fig. 8.3: Calibration of the fixed acoustic array using the old POSIDONIA system (VME). Red line = Ship's track; Blue dots = Detected transponder positions

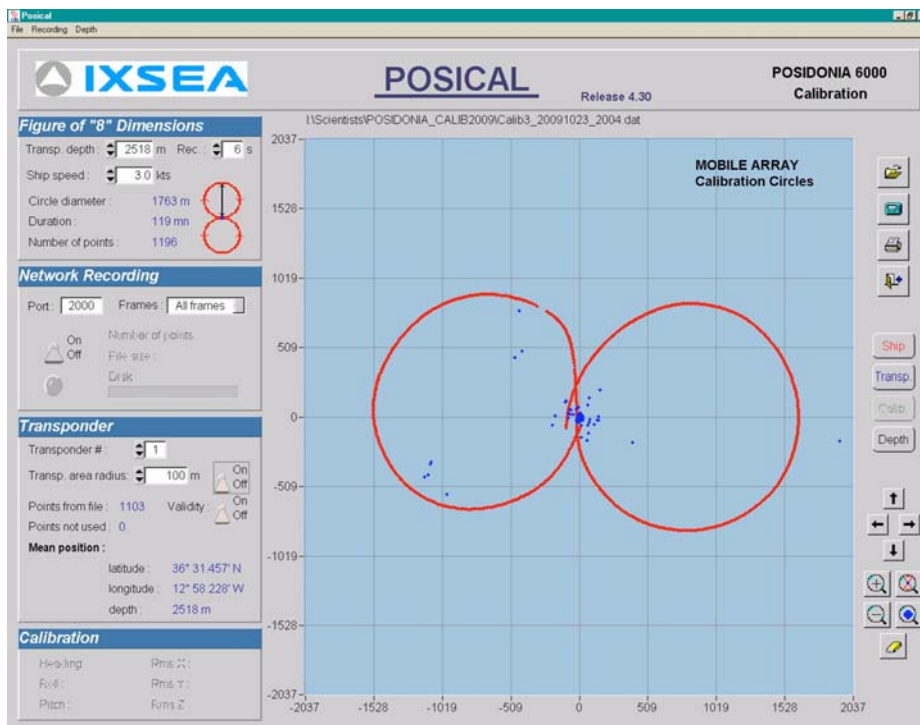


Fig.8.4: Calibration of the Mobile acoustic array using the old POSIDONIA System (VME).
 Red line = Ship's track; Blue dots = Detected transponder positions

9. OCCURRENCE, DISTRIBUTION AND ISOTOPIC COMPOSITION OF VOLATILE ORGANOHALOGENS ALONG A NORTH-SOUTH TRANSECT ALONG THE ATLANTIC OCEAN

Frank Laturus¹, Tanja Teschner¹
not on board: Enno Bahlmann¹, Richard
Seifert¹

¹IfBM

Introduction

The widespread use of chloro- and chlorofluorohydrocarbons (CFCs) and other volatile organohalogens in our industrialised society cause a large annual release of these compounds into the environment. Besides atmospheric pollution, some volatile organohalogens, for example chloroform, tri- and tetrachloroethene, also constitute a risk for the resources of drinking water as they can be transported to the groundwater from contaminated field sites or even from atmospheric deposition. These volatile organohalogens have been under scrutiny the recent years as they are a source for halogen radicals involved in various catalytic atmospheric reaction cycles, including the destruction of the stratospheric ozone layers. To avoid further depletion of the protecting ozone layer against solar ultraviolet radiation, the production and consumption of man-made ozone depleting substances is now controlled by international regulations (e.g. UNEP 1987). Besides the industrial emission, also natural emissions of volatile organohalogen compounds by several marine and terrestrial sources have been identified (e.g. Khalil et al. 1999, Laturus 2001, Laturus et al. 2002). Interesting is that extrapolations of global emissions of volatile organohalogens from natural sources into the atmosphere revealed source strengths comparable to the industrial input (e.g. McCulloch et al. 1999, Keene et al. 1999). For the terrestrial environment, several natural sources, such as wetlands, peatlands, salt marshes, rice fields, soil, forests, volcanos have been found to release mainly chlorinated compounds (e.g. Isidorov et al. 1990, Goodwin et al. 1995, Redeker et al. 2000, Yokouchi et al. 2002/2007, Laturus 2001, Laturus et al. 2002, Rhew et al. 2002, Scheeren et al. 2003, Manley et al. 2007, Gebhardt et al. 2008). Although the terrestrial environment is only 29 % of Earth's surface, it is a major contributor to the occurrence of methyl halides and other volatile reactive halogen-containing compounds in the environment. For example, salt marshes may contribute up to 20 % of the global methyl halide flux to the atmosphere (Rhew et al. 2002). However, those numbers are still rough estimates since many sources are only partially understood. A relevant source for volatile organohalogens too may be mangroves, recently found by a greenhouse experiment to produce chloromethane in substantial amounts (Manley et al. 2007). These plants cover approximately 60 - 70 % of the

tropical coastline, and may, thus, be central sources for methyl halides in the natural environment (Hogarth 1999). However, field studies on emissions of halomethanes from mangroves are still not available.

In the marine environment, the oceans are major sources for volatile organohalogens released into the atmosphere. However, the origin of these compounds inside the oceans has not yet been fully explored. At present, marine macroalgae and microalgae have been identified as a producer of volatile organohalogens. However, they are responsible for only 0.7 to 16 % of the total amount of volatile organohalogens annually emitted from the oceans. Thus, other so far unknown sources must still exist to balance the global halogen budget. Therefore, identification and quantification of marine sources and sinks of organohalogenes are a topic of particular interest.

Recently, signatures of carbon stable isotopes appeared to be a powerful tool to identify the dynamics of low molecular weight organohalogenes. Information from tool may allow to distinguish between different sources, to trace transport processes, and to estimate life time cycles of selected organohalogenes (Mead et al., 2008).

Objectives

The objectives of this project are to measure the concentrations and isotopic distribution of volatile organohalogens in air and surface water along a North-South transect from Bremerhaven, Germany, to Punta Arenas, Chile. Therefore, information on North-South distribution, on a biogenic or anthropogenic origin and on possible coastal impacts on volatile organohalogen concentrations in seawater and air can be determined.

The project will contribute to ongoing projects on studying the occurrence and distribution of volatile organohalogens at the West coast of Africa (SOPRAN) and Brazil (CliSAP). Furthermore, the project will deliver additional data to results of a West-East transect of the distribution of volatile organohalogens achieved during a cruise with the German research vessel *Meteor* (M78/2).

Work at Sea

Six times a day, the concentration of volatile organohalogens were measured in ambient air samples and in surface seawater. Ambient air was collected on the upper deck of the *Polarstern*, 30 m above seawater level against wind direction. The air was preconcentrated on a trap cold by liquid nitrogen and analysed for volatile organohalogens on board by gas chromatography. Simultaneously to the air sample, seawater was collected 10 m below surface by the ships own seawater collection system. The volatile organohalogens in the seawater sample were removed by helium and preconcentrated by liquid nitrogen before analysed by gas chromatography. Additionally, seawater was filtered to collect samples for the concentration of chlorophyll, which is an indication for the occurrence of microalgae known to emit volatile organohalogens. Besides the direct analysis of ambient air and

seawater for volatile organohalogenes, up to 400 L of ambient air was collected on special designed absorption tubes for the determination of the carbon stable isotopes signature. The analyses will be done by stable isotope mass spectrometry at the home laboratory in Hamburg.

Preliminary results

The sampling along the transect started after leaving the English Channel at $46^{\circ}16.4'N$, $8^{\circ}14.3'W$. The transect ended close to the Magellan Street at $48^{\circ}46.7'S$, $62^{\circ}0.6'W$. Fig. 9.1 shows the sampled transect, which consisted of a total of 105 sampling points. The first part of the transect up to $2^{\circ}16.98'N$, $35^{\circ}42.32'W$ went parallel to the coast of Spain and Northern Africa including the Canaric Islands and the Cape Verde islands to investigate possible influence of the terrestrial environment on the concentration of volatile halocarbon in air and surface water.

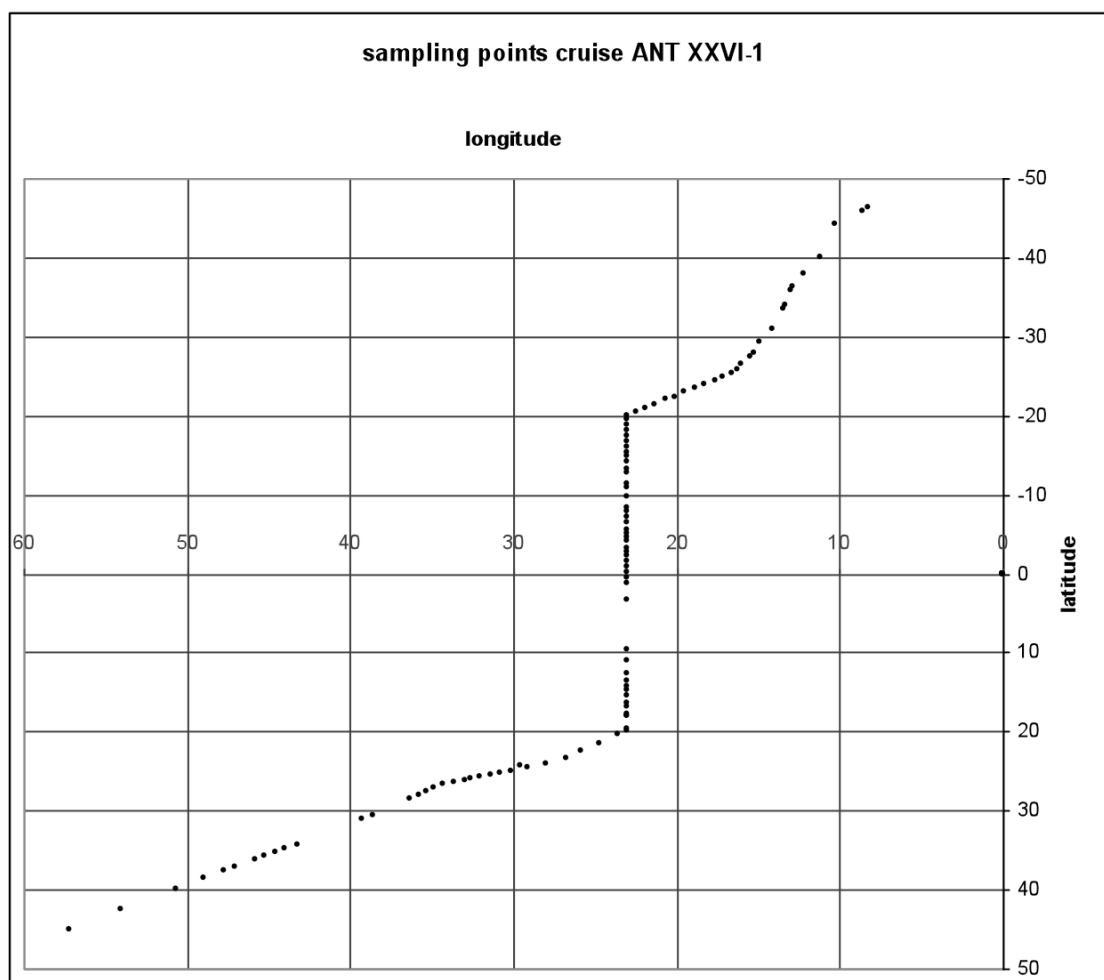


Fig. 9.1: Sampling points on cruise ANT-XXVI/1 for the determination of volatile organohalogenes in air and surface water of the Atlantic Ocean

The volatile organohalogen identified methyl iodide (CH_3I), chloroform (CHCl_3), bromochloromethane (CH_2BrCl), tetrachloromethane (CCl_4), trichloroethene (C_2HCl_3), dibromomethane (CH_2Br_2), bromodichloromethane (CHBrCl_2), chloriodomethane (CH_2ClI), tetrachloroethene (C_2Cl_4), dibromochloromethane (CHBr_2Cl), 1,2-dibromoethane (1,2-EtBr₂), bromoform (CHBr_3), and diiodomethane (CH_2I_2). Chlorophyll concentrations will be determined at the home laboratory first.

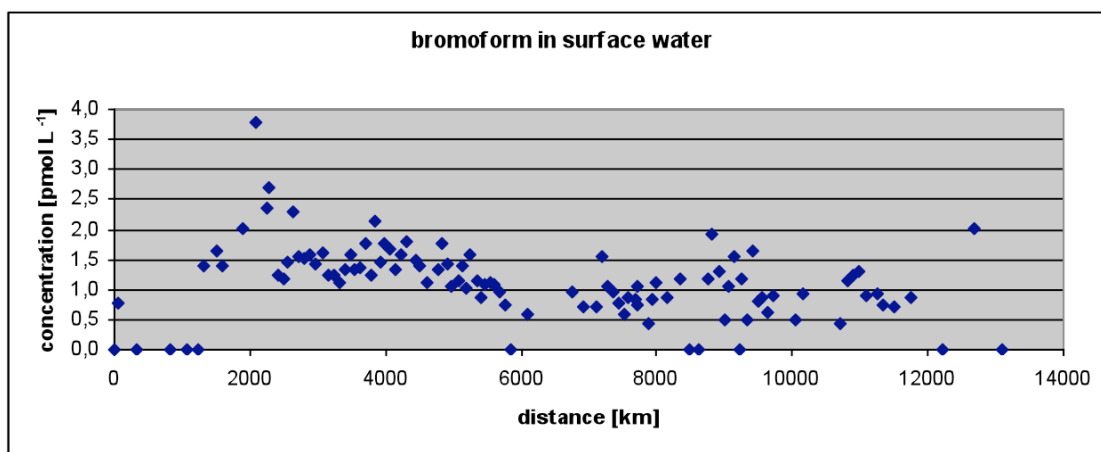


Fig. 9.2: Ambient air concentrations of bromoform (CHBr_3) along the North-South transect from Bremerhaven to Punta Arenas

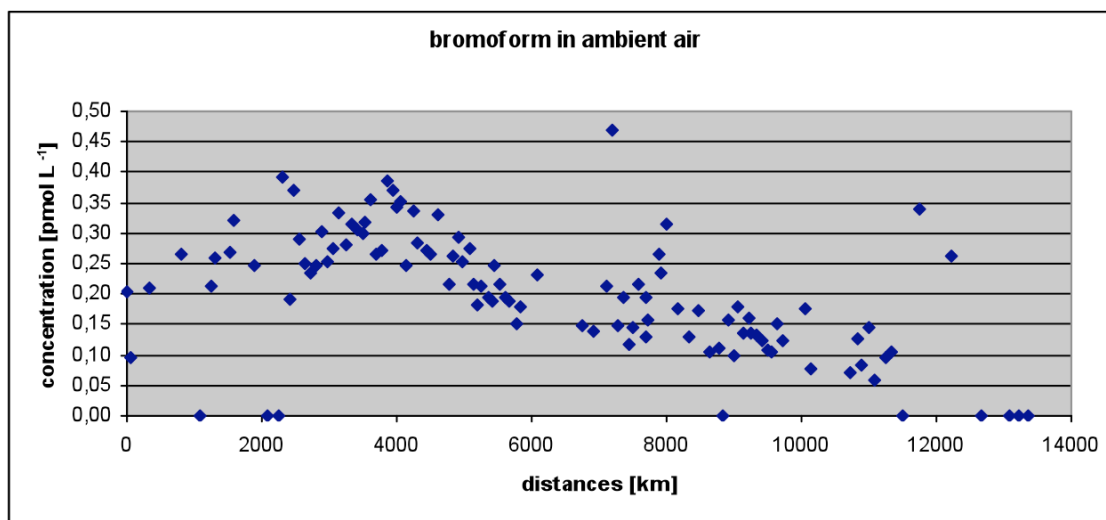


Fig. 9.3: Ambient air concentrations of bromoform (CHBr_3) along the North-South transect from Bremerhaven to Punta Arenas

The results for bromoform with its mainly natural sources in general showed a decrease of the air and seawater concentration from North to South (Fig. 9.2 and 9.3). A maximum of bromoform concentrations occurred close to the coast of North Africa possibly due to influences of coastal natural production and/or the strong Sarah dust event experienced during the cruise. The results from the isotope distribution of carbon-12 to carbon-13 in bromoform will allow a further estimation of its sources. A first view on the distribution of other volatile organohalogens detected revealed a similar distribution pattern. However, a detailed evaluation still has to be done before further results can be presented.

Conclusion

Natural sources have been found to be significant contributors to the input of volatile organohalogens to the environment. However, compared to industrial sources, natural sources can hardly be controlled. Thus, it is important to complete the picture of natural sources contributing to the environmental input of volatile organohalogens. It has been shown that changes of abiotic factors, such as nutrient concentration, temperature, salinity, ultraviolet radiation, can alter the release of volatile organohalogens by natural sources. Therefore, human influences on the environment resulting in eutrophication or further global warming can change the emission of volatile organohalogens by natural sources. For example, the investigations of marine macroalgae showed evidence for a significant increase in the release of these substances when the macroalgae are exposed to elevated levels of ultraviolet radiation. Therefore, increasing emission of volatile organohalogens may be expected in future from natural marine and terrestrial sources, when ultraviolet radiation levels reaching the Earth's surface still elevates due to a weakening stratospheric ozone layer. This would alter the global atmospheric input and in turn the stratospheric ozone chemistry, and has to be considered when predicting future scenarios in global climate changes.

References

- Gebhardt S, Colomb A, Hofmann R, Williams J, Lelieveld J (2008). Halogenated organic species over the tropical South American rainforest. *Atmos Chem Phys*, 8-12, 3185-3197.
- Goodwin KD, North WJ, Lidstrom ME (1997). Production of bromoform and dibromomethane by giant kelp: factors affecting release and comparison to anthropogenic bromine sources. *Limnol Oceanogr*, 42, 1725-1734.
- Hogarth PJ (1999). *The Biology of Mangroves*, Oxford Univ. Press, New York.
- Isidorov VA (1990). Organic chemistry of the Earth's atmosphere. Chapter 3 – Natural sources of organic components of the atmosphere. Springer, Berlin, 215p.
- Keene WC, et al. (1999). Composite global emissions of reactive chlorine from anthropogenic and natural sources – reactive chlorine emissions inventory. *J Geophys Res*, 104, 8429-8440.
- Khalil MAK, Morre RM, Harper DB, Lobert JM, Erickson DJ, Koropalov V, Sturges WT, Keene WC (1999). Natural emissions of chlorine-containing gases – reactive chlorine emissions inventory. *J Geophys Res*, 104, 8333-8346.

- Laternus F (2001). Marine macroalgae in Polar Regions as natural source of volatile organohalogen. *Environ Sci Pollut Res*, 8, 103-108.
- Laternus F, Haselmann KF, Borg T, Grøn C (2002). Terrestrial natural sources of trichloromethane (chloroform, CHCl₃) – an overview. *Biogeochemistry*, 60, 121-139.
- Manley SL, Wang NY, Walser ML, Cicerone RJ (2007). Methyl halide emissions from greenhouse grown mangroves. *Geophys Res Lett*, 34, L01806, doi:10.1029/2006GL027777.
- McCulloch A, Aucott ML, Benkovitz CM, Graedel TE, Kleiman G, Midgley PM, Li YF (1999). Global emissions of hydrogen chloride and chloromethane from coal combustion, incineration and industrial activities – reactive chlorine emissions inventory. *J Geophys Res*, 1004, 8391-8403.
- Mead M.I., Khan M.A.H., Bull I.D, White I.R., Nickless G., and Shallcross D.E. (2008). Stable carbon isotope analysis of selected halocarbons at parts per trillion concentration in an urban location. *Environmental Chemistry*, 5(5) 340–346.
- Redeker KR, Wang NY, Low JC, McMillan A, Tyler SC, Cicerone RJ (2000). Emissions of methyl halides from rice paddies. *Science* 290, 966-969.
- Rhew RC, Miller BR, Bill M, Goldstein AH, Weiss RF (2002). Environmental and biological controls on methyl halides emissions from southern California coastal salt marshes. *Biogeochemistry*, 60, 141-161.
- Scheeren HA et al. (2003). Measurements of reactive chlorocarbons over the Surinam tropical rain forest: indications for strong biogenic emissions. *Atmos Chem Phys Discuss*, 3, 5469–5512.
- UNEP (1987). The Montreal protocol on substances that deplete the ozone layer. United Nations Environmental Programme (UNEP) 192p.
- Yokouchi Y, Ikeda M, Inuzuka Y, Yukawa T (2002). Strong emission of methyl chloride from tropical plants. *Nature*, 416, 163-164.
- Yokouchi Y, Saito T, Ishigaki C, Aramoto M (2007). Identification of methyl chloride-emitting plants and atmospheric measurements on a subtropical island. *Chemosphere*, 69, 549–553.

10. AEROSOL REMOTE SENSING WITH FUBISS SUN AND SKY RADIOMETER

Jonas von Bismarck¹, Marco Starace¹,
Thomas Ruhtz¹

¹Institute for Space
Sciences, Freie Universität
Berlin

Objectives

Aerosol particles have an important impact on the surface net radiation budget by direct scattering and absorption (direct aerosol effect) of solar radiation, but also by providing cloud condensation nuclei (cloud albedo effect).

In addition to typical salt particles in the marine boundary layer, air masses over the Atlantic can contain a variety of different transported particle types originating from natural and anthropogenic sources on the surrounding continents, including dust particles from Saharan desert storms, soot particles from various combustion processes (e.g. forest fires in the African and American tropics and sub tropics) and sulphate droplets originating from industrial and volcanic sources.

In contrast to the ground based remote sensing of aerosols over land by stationary sun photometers as the AERONET stations, there is a lack of stationary platforms for comparable measurements on the ocean. Mounting aerosol remote sensing instruments on moving ships and using satellite measurements are the main approaches to fill this gap.

The FUBISS radiometers were originally designed for airborne remote sensing of aerosols and are therefore able to continuously correct their attitude when mounted on a moving ship in contrast to most stationary instruments. FUBISS-ASA2 is a combination of four multispectral radiometers on one platform which constantly points the entrance optics toward the sun. Two radiometers record the direct solar radiation in the UV/VIS and the NIR spectral region providing information about light extinction by aerosol particles. Furthermore two aureole adapters measure scattered sunlight in the 4° and 6° scattering angle region, containing information about the angular distribution of the radiation scattered by the aerosol particles, the so called phase function. FUBISS-ZENITH measures the sky radiance in the zenith extending the information about the aerosol phase function.

Work at Sea

The controlling unit, the data logging PC and the power supply have been mounted inside the crow's nest (the observation tower) aboard *Polarstern*. The FUBISS radiometers ASA2 and ZENITH (Fig. 10.1) and the controlling/monitoring laptop were set up on the terrace of the crow's nest between dawn and dusk on days with

acceptable measuring conditions; meaning no or only partial cloud cover and zero precipitation.

The sun and aureole photometer position had to be changed a few times every day when the terrace roof moved into the line of sight of the instrument. Attitude changes of the ship (e.g. due to the sea state) and the apparent motion of the sun are compensated for with 10 Hz using DC-motor driven round-stages, which are controlled by the signal of a 4-quadrant-diode.

Correction of the misalignment of the measured ZENITH radiances due to the motion of the platform is facilitated by data from the *MINS SCIENTIFIC NAVIGATION PLATFORM* aboard *Polarstern*. Marking of the data points influenced by the smoke-track of the ship is performed using relative wind directions provided by the onboard weather station.

To adapt sensor integration time and document cloud cover conditions, the instruments were supervised during measurement. Processing of raw data was performed on standard laptops aboard the ship.

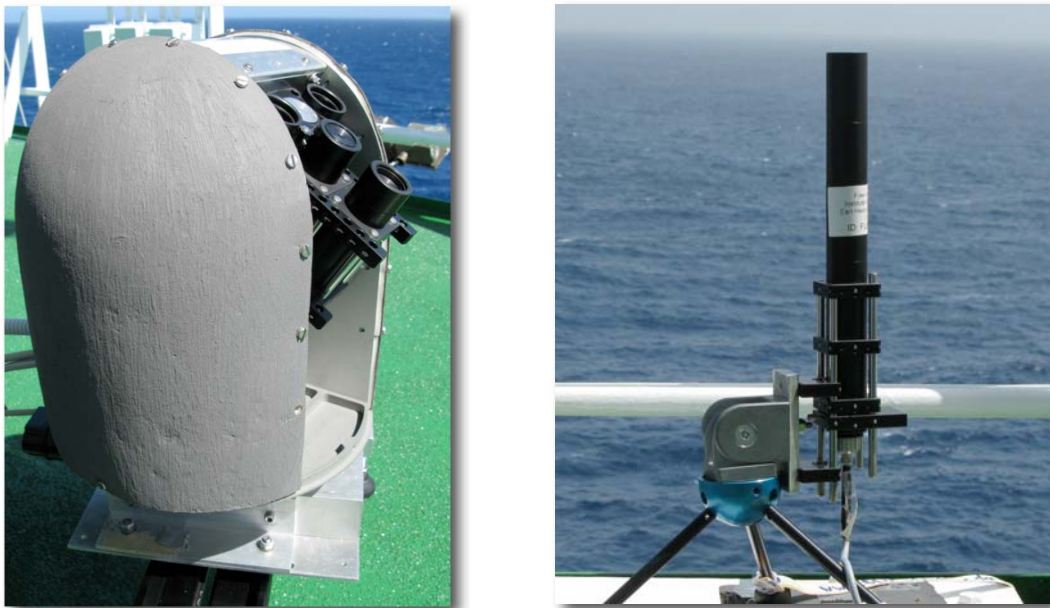


Fig. 10.1: The FUBISS radiometer ASA2 (left) and ZENITH (right).
Photographs by Jonas von Bismarck

Results

Over all more than 150 hours of multispectral (300 nm - 1,600 nm) sun and sky radiances could be recorded with a rate of about 10 Hz on 22 days spread over the whole cruise leg from Bremerhaven to Punta Arenas, of which measurements with direct sunlight are processed. Data was recorded on days with a variety of different

atmospheric conditions, such as a Saharan dust outbreak over the Cape Verde Islands, typical marine conditions with salt particles in the marine boundary layer and pristine conditions in the southern Atlantic.

Column based products derived directly from the measured radiances include the aerosol optical depth, the Ångström exponent, the slope of the aerosol phase function in the forward scattering direction. This allowed conclusions about the size distribution and type of aerosol particles.

The high precision of these aerosol optical properties allow the validation of products derived from measurements of overpassing satellites. A comparison of the aerosol optical depths during the Saharan dust outbreak derived from FUBISS-ASA2 and the handheld MICROTOS sun photometer operated synchronously aboard *Polarstern* is shown in Fig. 10.2. Furthermore, the column integrated ozone concentration is derived from the sun photometer data.

Including the measured zenith radiances, inverse modelling with the radiative transfer model MOMO at the Institute for Space Sciences will allow further conclusions about microphysical properties of the aerosol and about the effect of the measured particles on the net radiation budget.

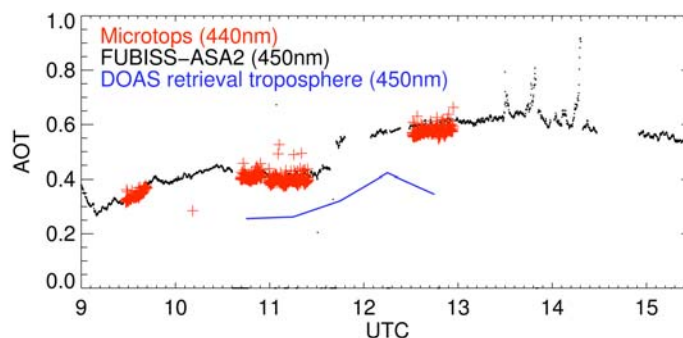


Fig. 10.2: Aerosol optical thickness on the 31 Oct 2009 measured from *Polarstern*

11. DIVERSITY AND ACTIVITY OF DIAZOTROPHIC CYANOBACTERIA

Harald Schunck¹, Tina Baustian¹
not on board: Julie LaRoche¹

¹ IFM-GEOMAR

Objectives

Diazotrophic organisms are prokaryotes which have the unique ability of converting molecular Nitrogen (N₂) into Ammonia (NH₄⁺), a process also known as nitrogen fixation. Since NH₄⁺ is readily assimilated also by other organisms, nitrogen fixation is an important input process of bioavailable (fixed) nitrogen into the ocean. This input is counteracted by the removal of fixed nitrogen through anaerobic ammonia oxidation (ANAMMOX) and denitrification.

Global rate estimates of these input and removal processes in the ocean do not balance and suggest a net loss of fixed nitrogen from the ocean. However, since most parts of the world's ocean are still undersampled with regards to marine diazotrophs and nitrogen fixation rates, one reason for the estimated imbalance may be this paucity of data.

Therefore the main objective of this project is to determine abundance, diversity and activity of diazotrophic microorganisms as well as bulk primary production rates.

The samples collected on this cruise will be analyzed using molecular biological methods: Different phylotypes of diazotrophs will be detected and quantified by sequence analysis of the *nifH* gene, which encodes a highly conserved subunit of the nitrogenase enzyme. Previous studies on marine diazotrophs using molecular biological methods have led to the discovery of many new species, especially in the unicellular fraction. Molecular biological methods could therefore deepen the understanding of the marine nitrogen cycle and potentially close existing gaps in the global marine nitrogen budget.

A similar study to this one had been conducted on the *Polarstern* ANT-XXIV/4 cruise in the northern hemisphere spring 2008. Because the timing of ANT-XXVI/1 is in northern hemisphere fall, one goal is to observe whether or not the trends found between the North and South Atlantic can still be found in the current cruise, or if the different times of year on both hemispheres have an effect on these trends.

Work at sea

For investigations of the surface ocean, discrete seawater samples were taken every 8 h from a depth of 10 m for analysis of *nifH* sequences as well as for analytical flow cytometry and nutrient concentrations. Additionally, samples for measurements of carbon and nitrogen fixation rates as well as POC, PON and POP were taken every 16 h.

To assess the composition of the diazotrophic community within deeper water layers depth profiles were conducted at 7 stations (40°N, 20°N, 10°N, 0°, 20°S, 30°S, 40°S) using a CTD water sampler. *nifH* sequence analysis-, analytical flow cytometry- and nutrient samples were taken at 6 depths between 5 and 450 m.

Samples for *nifH* analysis as well as POC, PON and POP were filtered on board. Samples for analytical flow cytometry were conserved with glutaraldehyde.

For the determination of carbon and nitrogen fixation rates stable isotopes (^{13}C and ^{15}N) were added to bottled water samples which were subsequently incubated in a microcosm for 24 hours (Fig. 11.1). All samples were frozen for later analysis.



Fig. 11.1: Microcosm for the incubation of bottled water samples used for the assessment of carbon and nitrogen fixation rates. Via the microcom temperature and light- conditions of about 10 m water depth were simulated. Photograph by Tina Baustian

Preliminary results

For the quantitative abundance estimates of *nifH* phylotypes 200 DNA samples were collected. Additionally, 200 RNA samples for quantitative PCR-studies of the *nifH* gene were taken throughout the transect. For cell counts of diazotrophs and the associated microbial community via analytical flow cytometry 300 samples were conserved. For the analysis of nitrogen fixation and primary production of the microbial community from surface waters a total of 50 incubations were carried out during ANT-XXVI/1, including 50 samples each for the determination of POC, PON and POP. Furthermore, 150 samples for the measurement of nutrient concentrations were taken.

References

- Langlois RJ, La Roche J, Raab PA (2005). Diazotrophic Diversity and Distribution in the Tropical and Subtropical Atlantic Ocean. *Applied and Environmental Microbiology*, 71 (12): 7910-7919.
- Langlois RJ, Hümmer D, La Roche J (2008). Abundances and Distributions of the Dominant *nifH* Phylotypes in the Northern Atlantic Ocean. *Applied and Environmental Microbiology*, 74 (6): 1922-1931.
- Grefe, I (2008). Latitudinal Distribution, Abundance and Activity of Marine Diazotrophs. Diplomarbeit, IFM-GEOMAR, Leibniz Institut für Meereswissenschaften an der Mathematisch-Naturwissenschaftlichen Fakultät der Christian-Albrechts Universität zu Kiel.

12. PARASOUND: SYSTEM TESTING AND TRAINING UNDER EXPEDITION CONDITIONS – INSTALLATION OF VIDEO GRAB AND MSCL

Gerhard Kuhn¹, Grit Freiwald¹, Sze-Ling Ho¹, Helmut Kawohl¹, Johann Phillipp Klages¹, Frank Lamy¹, Ansa Lindeque¹, Conny Walther¹

¹Alfred-Wegener-Institut, Bremerhaven

Background

Sea floor and sub-bottom reflection patterns obtained by the deep sea sediment echo sounder PARASOUND (ATLAS HYDROGRAPHIC, Bremen, Germany) characterize the uppermost sediments of the ocean in terms of their acoustic behaviour down to about 200 m below the sea floor. This can be used to study depositional environments on larger scales in terms of space and time and to identify suitable coring locations. On ANT-XXVI/1 the area at sea along the routine course track from Bremerhaven to Las Palmas is particularly suitable for PARASOUND system testing and training because the range of sea-floor topography, sediment penetration and water depth (shallow water to more than 5,000 m) allows using all possible modes of operation.

The parametric system PARASOUND was upgraded from DS II to DS III-P70 in May 2007, which included a complete installation of new hardware and software and replacement of the original system installed on *Polarstern* in 1989. From June 2007 to May 2009 four sea-trial phases including software updating and testing at sea (ARK-XXII/1a, ANT-XXIV/1, ANT-XXIV/4, ANT-XXV/5b), as well as three expeditions using the new system in preliminary modes were carried out (ARK-XXII/2, ARK-XXIII/3, ARK-XXIV/3). The technical specifications of the upgraded system, the new functions as well as technical problems are described in the cruise reports of the legs above.

Objectives

There are the following objectives for using PARASOUND on ANT-XXVI/1:

- to update the system with new software versions,
- to test the system for different operational modes,
- to train six students for self-efficient operation of the new PARASOUND system P-70.

The update and test became necessary after problems occurred for transmission modes „Pulse Train“ and „Quasi-Equidistant“ and insufficient depth detection and system stability on cruise leg ANT-XXV/5b.

The training course is part of the education for graduate students of the Helmholtz Graduate School for Polar and Marine Research POLMAR and Earth System Science Research School ESSReS at AWI. Aim of the lecture was to learn how to handle a complex data acquisition system, data storage and management and geological interpretation of sea floor structures. Furthermore it will ensure sufficient PARASOUND surveys for geological projects carried out on forthcoming expeditions of the *Polarstern*, *Maria S. Merian* and *Sonne* in 2010 - 2011, where some students will participate and PARASOUND has to be used.

Work at Sea

On October 16, when the group of 7 persons came on board in Bremerhaven to work with the PARASOUND system, a soft- and hardware update was carried out by Jörn Ewert from Atlas Hydrographic. The new installation included new hard disks (500 GB) for the operator- and data-PCs, printing via printer server, new installation of Windows XP system and driver software, CM V 1.38.45, AHS V 2.1.0, AHC V 2.2.4, and Parastore V 3.3.2. After a brief system check Jörn Ewert left the ship in the evening of the same day.

The remaining group used the system during 24-hour operation per day under expedition conditions. PARASOUND was switched off on October 26, the evening before approaching Las Palmas. Data acquisition and temporary storage was for testing and training purposes only. No survey or research was carried out.

With the updates the system stability (both Hydromap Control and Parastore) was increased significantly. Hydromap Control had no and Parastore some crashes of unknown reasons. Autonomous depth detection with PHF now is one possible mode for stable system operation. A problem was encountered with erroneous delay and ships draught offset in saved PS3 and SEG-Y data. Therefore an updated Parastore V 3.3.5 was installed and tested on 25 October. Now the PS3 and SEG-Y files are saved with the right delay. Operation of the system in quasi-equidistant mode produces Parastore crashes if the sea floor topography is too steep. Here a manual mode and depth control and a single pulse or a low pulse train mode could be more successful, but we have had no more possibilities to test this. To protect the Parasound PCs against computer viruses the IT-manager installed all necessary system updates and antivirus software.

The training course included knowledge about the system, switching the system off and on, watch keeping, depth control, working with different modes of pulse transmission, data acquisition, storage, printing, data visualization, processing, replay and data management. The participants were trained to operate the system self

efficiently, learned first geological interpretation of seafloor structures and were prepared for trouble shooting.

The documentations on “Parasound data storage”, “Parasound switch on” and the “Handbuch für Parasound” were updated.

Conclusions

The new software versions revealed significant improvement of the PARASOUND system on *Polarstern*. Over longer profile segments it is fully operational and runs up to two days (before the update) without crashes. It seems that after the update it is less stable and Parastore crashes more often, but in the short time left we could not test this sufficiently. The participants of the PARASOUND course consider the training a success and as very useful for preparing PARASOUND operators prior to expeditions.

13. ACKNOWLEDGEMENT

We like to thank AWI for the support for preparing, executing, and finalizing the scientific work of this cruise. We thank Master Pahl and his crew for the support and the nice working atmosphere on board.

We are grateful to Frauke Nevoigt at IFM-GEOMAR for her editorial work in preparing this final report.

During the cruise we had received the sad announcement of the sudden and unexpected death of Dr. Sönke Neben from AWI. Sönke Neben was responsible for the logistics of the scientific operations on board, and many of us have enjoyed working together with him in preparing the current expedition. Our thoughts and deepest sympathy are with his family.

APPENDIX

A.1 PARTICIPATING INSTITUTIONS

A.2 CRUISE PARTICIPANTS

A.3 SHIP'S CREW

A.4 STATION LIST

A.1 TEILNEHMENDE INSTITUTE / PARTICIPATING INSTITUTIONS

	Adresse Address
AWI	Alfred-Wegener-Institut für Polar- und Meeresforschung in der Helmholtz-Gemeinschaft Postfach 120161 27515 Bremerhaven, Germany
DFG-SKO	Senatskommission für Ozeanographie der DFG Am Handelshafen 12 27570 Bremerhaven, Germany
CAU	Christian-Albrechts-Universität zu Kiel Christian-Albrechts-Platz 4 24118 Kiel, Germany
DWD	Deutscher Wetterdienst Geschäftsbereich Wettervorhersage Seeschiffahrtsberatung Bernhard Nocht Str. 76 20359 Hamburg, Germany
DWD-MM	Deutscher Wetterdienst (DWD) TI 33 A4 - Maritimes Messnetz Frahmredder 95 22393 Hamburg, Germany
GKSS	GKSS Research Center Max-Planck-Straße 1 21502 Geesthacht, Germany
HATLAPA	Uetersener Maschinenfabrik GmbH & Co. KG Tornescher Weg 5-7 25436 Uetersen, Germany
IfBM	Institute for Biogeochemistry and Marine Chemistry University of Hamburg, Bundesstrasse 55, 20146 Hamburg, Germany

Adresse
Address

IfT	Institute for Tropospheric Research Permoserstraße 15 04318 Leipzig, Germany
IfW-FU-Berlin	Institut für Weltraumwissenschaften - Freie Universität Berlin Carl-Heinrich-Becker-Weg 6-10 12165 Berlin, Germany
IFM-GEOMAR	Leibniz-Institute for Marine Sciences Düsternbrooker Weg 20 24105 Kiel, Germany
IXSEA	IXSEA Rue Rivoalon Sainte-Anne du Portzic 29200 Brest, France
Laeisz	Reederei F. Laeisz (Bremerhaven) GmbH Brückenstraße 25 27568 Bremerhaven, Germany
RF	RF Forschungsschiffahrt GmbH Blumenthalstr. 15 28209 Bremen, Germany
ZMAW	Zentrum für Meeres- und Klimaforschung (ZMK) Bundesstrasse 53, 20146 Hamburg, Germany
ZMK	Universität Hamburg, Zentrum für Meeres- u. Klimaforschung Leitstelle METEOR / MERIAN Bundesstrasse 53 20146 Hamburg, Germany

A.2 FAHRTTEILNEHMER / CRUISE PARTICIPANTS

Name/ Last name	Vorname/ First name	Institut/ Institute	Beruf/ Profession
Aßmann	Steffen	IFM-GEOMAR, GKSS	Chemical Engineer
Baustian	Tina	IFM-GEOMAR	Student, biology
Bohlmann	Harald	ISITEC	Electronic Engineer
Bumke	Karl	IFM-GEOMAR	Meteorologist
El Naggar	Saad	AWI	Physicist
Fietzek	Peer	IFM-GEOMAR	Physicist, marine chemist
Freiwald	Grit	AWI	Mathematician
Gehrung	Martina	GKSS	Engineer
Hieronymi	Martin	IFM-GEOMAR	Offshore Engineer
Heus	Thijs	ZMAW	Meteorologist
Ho	Sze-Ling	AWI	Student, geology
Hollstein	Andre	IfW-FU-Berlin	Physicist
Kalisch	John	IFM-GEOMAR	Meteorologist
Kanitz	Thomas	IfT	Physicist
Kawohl	Helmut	AWI	
Klages	Johann Phillipp	AWI	
Kleta	Henry	DWD-MM	Engineer
Kuhn	Gerhard	AWI	Geologist
Lamy	Frank	AWI	Geoscientist
Laternus	Frank	IfBM	Marine chemist
Lehmenhecker	Sascha	AWI	Engineer
Lindeque	Ansa	AWI	Geophysicist
Löffler	Sonja-B.	DFG-SKO	Geologist
Macke	Andreas	IFM-GEOMAR	Chief Scientist
Ohm	Thomas	ZMK	Engineer
Pluder	Andreas	Laeisz	Technical Superintendent
Rogenhagen	Johannes	Fielax/ Laeisz	Project Manager
Roger	Dominique	IXSEA	Engineer
Rohardt	Gerd	AWI	Oceanographer
Schunck	Harald	IFM-GEOMAR	Biological Oceanographer
Sablotny	Burkhard	AWI	Engineer
Sonnabend	Hartmut	DWD	Technician
Starace	Marco	IfW-FU-Berlin	Student, physics
Teschner	Tanja	IfBM	Student
von Bismarck	Jonas	IfW-FU-Berlin	Physicist
Walther	Conny	AWI	Physicist
Weber	Hannah	IFM-GEOMAR	Student, biology
Werner	Reinhard	IFM-GEOMAR	Geologe
Zoll	Yann	IFM-GEOMAR	Meteorologist
Rex	Andreas	RF Forschungsschiffahrt	Chief Engineer FS Sonne
Schrapel	Andreas	RF Forschungsschiffahrt	Boatswain FS Sonne

A.3 SCHIFFSBESATZUNG / SHIP'S CREW

No.	Name	Rank
1.	Pahl, Uwe	Master
2.	Ettlin, Margrith	1. Offc.
3.	Krohn, Günter	Ch.Eng.
4.	Fallei, Holger	2. Offc.
5.	Janik, Michael	2. Offc.
6.	Pohl, Claus	Doctor
7.	Hecht, Andreas	R.Offc.
8.	Minzlaff,Hans-Ulrich	2. Eng.
9.	Sümnicht, Stefan	2. Eng.
10.	Kotnik, Herbert	3. Eng.
11.	Scholz, Manfred	ElecEng.
12.	Muhle, Helmut	ELO
13.	Dimmler, Werner	ELO
14.	Feiertag, Thomas	ELO
15.	Winter, Andreas	ELO
16.	Loidl, Reiner	Boatsw.
17.	Reise, Lutz	Carpenter
18.	Bäcker, Andreas	A.B.
19.	Guse, Hartmut	A.B.
20.	Hagemann, Manfred	A.B.
21.	Pousada Martinez, S.	A.B.
22.	Scheel, Sebastian	A.B.
23.	Schmidt, Uwe	A.B.
24.	Wende, Uwe	A.B.
25.	Winkler,Michael	A.B.
26.	Preußner, Jörg	Storek.
27.	Elsner, Klaus	Mot-man
28.	Pinske, Lutz	Mot-man
29.	Schütt, Norbert	Mot-man
30.	Teichert, Uwe	Mot-man
31.	Voy, Bernd	Mot-man
32.	Müller-Homburg, R.-	Cook
33.	Silinski, Frank	Cooksmate
34.	Martens, Michael	Cooksmate
35.	Jürgens, Monika	1.Stwdess
36.	Wöckener, Martina	Stwdss/Krankenschwester
37.	Czyborra, Bärbel	2.Stwdess
38.	Gaude, Hans-Jürgen	2.Steward
39.	Huang, Wu-Mei	2.Steward
40.	Silinski, Carmen	2.Stwdess
41.	Möller, Wolfgang	2.Steward

No.	Name	Rank
42.	Yu, Kwok Yuen	Laundrym.
43.	Apel, Rodney	Trainee
44.	Stronzek, David	Trainee/E

A.4 STATIONSLISTE / STATION LIST PS 75

Station PS75	Date	Time (start)	Time (end)	Position (Lat.)	Position (Lon.)	Depth (m)	Gear
0001-1	19.10.	08:36	09:02	47° 30.55' N	6° 56.00' W	360	CTD/Rosette
0001-2	19.10.	09:07	09:54	47° 30.58' N	6° 55.99' W	150	Releaser
0001-3	19.10.	10:52	11:35	47° 30.75' N	6° 56.41' W	359	Video camera
0002-1	20.10.	12:08	12:23	44° 0.19' N	10° 30.72' W	203	CTD/Rosette
0002-2	20.10.	12:30	20:03	43° 59.85' N	10° 30.07' W	3112	Test LWL-Winde
0003-1	21.10.	18:14	20:08	40° 0.24' N	11° 11.24' W	1046	CTD-CO2/Ros.
0004-1	22.10.	12:08	12:27	37° 17.41' N	12° 24.50' W	45	Ramses
0004-2	22.10.	12:34	17:43	37° 17.78' N	12° 24.57' W	1025	CTD-CO2/Ros.
0004-3	22.10.	18:01	21:14	37°17.54' N	12° 23.49' W	5211	CTD/Rosette
0004-4	22.10.	21:23	22:38	37° 18.57' N	12° 23.31' W		Lichtwellenleiter
0005-1	23.10.	04:25	06:21	36° 31.84' N	12° 59.19' W	2693	CTD/Rosette
0005-2	23.10.	06:38	06:45	36° 31.48' N	12° 59.35' W		Mooring 5 floats
0005-3	23.10.	07:44	13:02	36° 31.14' N	12° 59.59' W		Posidonia
0005-4	23.10.	13:18	13:56	36° 33.52' N	12° 56.54' W	1000	Test LWL-Winde
0005-5	23.10.	14:03	16:54	36° 35.01' N	12° 54.65' W	2650	Test LWL-Winde
0005-6	23.10.	17:48	19:32	36° 33.44' N	12° 56.62' W	2466	Video-camera
0005-7	23./24.10.	20:02	07:32	36° 31.45' N	12° 58.57' W		Posidonia
0005-8	24.10.	07:24	08:12	36° 31.48' N	12° 59.20' W		Mooring
0005-9	24.10.	08:27	10:18	36° 30.36' N	12° 58.54' W		Test LWL-Winde
0005-10	24.10.	10:35	10:53	36° 30.29' N	12° 58.36' W		Video/Backengr
0005-11	24.10.	11:07	11:21	36° 30.32' N	12° 58.30' W	202	CTD/Rosette
0006-1	24./25.10.	18:17	03:00	35° 35.02' N	13° 14.94' W		Hydro Sweep ParaSound
0007-1	25.10.	13:04	13:45	33° 40.70' N	13° 30.88' W		Zodiak
0007-2	25.10.	13:06	13:45	33° 40.70' N	13° 30.98' W	45	Ramses
0007-3	25.10.	13:52	14:10	33° 40.71' N	13° 30.94' W	200	CTD/Rosette
0008-1	25.10.	18:50	22:48	32° 56.67' N	13° 18.58' W		HydroSweep/ Parasound
0009-1	26.10.	13:02	13:48	30° 17.35' N	14° 21.34' W		Zodiak
0009-2	26.10.	13:03	13:46	30° 17.29' N	14° 21.00' W	45	Ramses
0009-3	26.10.	13:10	13:29	30° 17.31' N	14° 21.23' W	202	CTD/Rosette
0010-1	28.10.	13:02	13:50	25° 43.63' N	16° 22.10' W		Zodiak
0010-2	28.10.	13:03	13:45	25° 43.68' N	16° 22.19' W	45	Ramses
0010-3	28.10.	13:08	13:25	25° 43.64' N	16° 22.12' W	204	CTD/Rosette
0011-1	30.10.	13:04	14:20	19° 44.23' N	22° 59.80' W		Zodiak
0011-2	30.10.	13:07	13:49	19° 44.07' N	22° 59.82' W	45	Ramses
0011-3	30.10.	13:08	14:17	19° 44.04' N	22° 59.83' W	1018	CTD/Rosette/Bio
0012-1	31.10.	13:04	13:56	15° 43.39' N	22° 59.81' W		Zodiak
0012-2	31.10.	13:08	13:51	15° 43.27' N	22° 59.95' W	45	Ramses
0012-3	31.10.	13:12	13:24	15° 43.32' N	22° 59.84' W	115	CTD/Rosette
0013-1	01.11.	14:04	14:56	11° 49.69' N	22° 59.76' W		Zodiak
0013-2	01.11.	14:08	14:51	11° 49.78' N	22° 59.83' W	45	Ramses
0013-3	01.11.	14:13	14:29	11° 49.71' N	22° 59.80' W	202	CTD/Rosette
0014-1	02.11.	02:23	02:54	10° 0.21' N	23° 0.23' W	458	CTD/Rosette/Bio
0015-1	03.11.	14:02	14:51	4° 54.83' N	23° 0.06' W		Zodiak
0015-2	03.11.	14:05	14:48	4° 54.49' N	23° 0.20' W	45	Ramses

Station PS75	Date	Time (start)	Time (end)	Position (Lat.)	Position (Lon.)	Depth (m)	Gear
0001-1	19.10.	08:36	09:02	47° 30.55' N	6° 56.00' W	360	CTD/Rosette
0015-3	03.11.	14:08	14:28	4° 54.64' N	23° 0.13' W	204	CTD/Rosette
0016-1	04.11.	09:03	13:56	2° 34.43' N	22° 59.85' W	1019	CTD-CO2/Ros.
0016-2	04.11.	14:04	14:46	2° 33.91' N	22° 59.57' W		Zodiak
0016-3	04.11.	14:06	14:41	2° 33.87' N	22° 59.53' W	20	Ramses
0017-1	05.11.	13:06	13:40	0° 1.23' S	23° 0.15' W	461	CTD/Rosette/Bio
0018-1	06.11.	14:00	14:44	3° 54.09' S	23° 0.17' W		Zodiak
0018-2	06.11.	14:06	14:38	3° 54.11' S	23° 0.39' W	10	Ramses
0018-3	06.11.	14:10	14:28	3° 54.12' S	23° 0.37' W	208	CTD/Rosette
0019-1	07.11.	14:05	15:16	7° 48.52' S	23° 0.02' W		Zodiak
0020-1	08.11.	14:01	14:53	11° 36.56' S	23° 0.07' W		Zodiak
0020-2	08.11.	14:05	14:49	11° 36.41' S	23° 0.25' W	45	Ramses
0020-3	08.11.	14:09	14:24	11° 36.54' S	23° 0.15' W	205	CTD/Rosette
0021-1	10.11.	14:03	14:46	19° 44.64' S	22° 59.96' W		Zodiak
0021-2	10.11.	14:05	14:42	19° 44.69' S	22° 59.82' W	45	Ramses
0021-3	10.11.	14:10	15:13	19° 44.67' S	22° 59.89' W	1024	CTD/Ros./Bio
0022-1	11.11.	15:03	16:03	22° 34.44' S	25° 50.96' W		Zodiak
0022-2	11.11.	15:13	15:59	22° 34.68' S	25° 51.41' W	45	Ramses
0022-3	11.11.	15:14	15:30	22° 34.53' S	25° 51.21' W	200	CTD/Rosette
0023-1	12.11.	15:02	15:48	24° 32.84' S	29° 8.44' W		Zodiak
0023-2	12.11.	15:07	15:43	24° 33.18' S	29° 8.53' W	45	Ramses
0023-3	12.11.	15:11	15:29	24° 33.02' S	29° 8.52' W	203	CTD/Rosette
0024-1	13.11.	15:02	16:03	26° 3.49' S	32° 43.76' W		Zodiak
0024-2	13.11.	15:06	15:44	26° 3.66' S	32° 44.20' W	45	Ramses
0024-3	13.11.	15:09	15:23	26° 3.55' S	32° 43.99' W	205	CTD/Rosette
0025-1	14.11.	02:37	05:47	26° 41.10' S	34° 13.37' W	4895	CTD/Rosette
0026-1	15.11.	15:03	15:51	30° 27.31' S	38° 27.95' W		Zodiak
0026-2	15.11.	15:08	15:44	30° 27.35' S	38° 27.95' W	45	Ramses
0026-3	15.11.	15:13	15:46	30° 27.33' S	38° 27.94' W	458	CTD/Rosette/Bio
0027-1	15./16.11.	22:50	01:35	31° 11.80' S	39° 18.92' W	4457	CTD/Rosette
0028-1	16.11.	15:00	15:51	32° 38.22' S	41° 6.48' W		Zodiak
0028-2	16.11.	15:04	15:47	32° 38.16' S	41° 6.69' W	45	Ramses
0028-3	16.11.	15:07	15:24	32° 38.23' S	41° 6.59' W	202	CTD/Rosette
0029-1	17.11.	12:36	13:31	34° 49.84' S	43° 53.59' W		Zodiak
0029-2	17.11.	12:38	13:19	34° 49.50' S	43° 53.73' W	45	Ramses
0029-3	17.11.	12:41	12:57	34° 49.78' S	43° 53.69' W	202	CTD/Rosette
0030-1	19.11.	12:08	19:23	39° 56.75' S	50° 41.04' W	2054	CTD-CO2/Bio
0031-1	20.11.	10:07	15:14	41° 38.15' S	52° 47.67' W	1000	CTD-CO2/Ros.
0031-2	20.11.	15:20	16:10	41° 37.43' S	52° 51.97' W		Zodiak
0031-3	20.11.	15:24	16:01	41° 36.90' S	52° 51.97' W	45	Ramses
0032-1	21.11.	15:05	15:49	44° 28.52' S	56° 18.96' W		Zodiak
0032-2	21.11.	15:10	15:45	44° 29.47' S	56° 18.53' W	45	Ramses
0032-3	21.11.	15:13	15:30	44° 29.05' S	56° 18.89' W	202	CTD/Rosette
0033-1	22.11.	16:06	16:54	47° 19.45' S	60° 0.14' W		Zodiak
0033-2	22.11.	16:10	16:50	47° 19.32' S	60° 0.29' W	45	Ramses
0033-3	22.11.	16:14	16:30	47° 19.37' S	60° 0.25' W	202	CTD/Rosette

Die "Berichte zur Polar- und Meeresforschung" (ISSN 1866-3192) werden beginnend mit dem Heft Nr. 569 (2008) ausschließlich elektronisch als Open-Access-Publikation herausgegeben. Ein Verzeichnis aller Hefte einschließlich der Druckausgaben (Heft 377-568) sowie der früheren "**Berichte zur Polarforschung**" (Heft 1-376, von 1982 bis 2000) befindet sich im Internet in der Ablage des electronic Information Center des AWI (**ePIC**) unter der URL <http://epic.awi.de>. Durch Auswahl "Reports on Polar- and Marine Research" auf der rechten Seite des Fensters wird eine Liste der Publikationen in alphabetischer Reihenfolge (nach Autoren) innerhalb der absteigenden chronologischen Reihenfolge der Jahrgänge erzeugt.

To generate a list of all Reports past issues, use the following URL: <http://epic.awi.de> and select the right frame to browse "Reports on Polar and Marine Research". A chronological list in declining order, author names alphabetical, will be produced, and pdf-icons shown for open access download.

Verzeichnis der zuletzt erschienenen Hefte:

Heft-Nr. 602/2009 — "Cumacea (Crustacea; Peracarida) of the Antarctic shelf – diversity, biogeography, and phylogeny", by Peter Rehm

Heft-Nr. 603/2010 — "The Expedition of the Research Vessel 'Polarstern' to the Antarctic in 2009 (ANT-XXV/5)", edited by Walter Zenk and Saad El Nagggar

Heft-Nr. 604/2010 — "The Expedition of the Research Vessel 'Polarstern' to the Antarctic in 2007/2008 (ANT-XXIV/2)", edited by Ulrich Bathmann

Heft-Nr. 605/2010 — "The Expedition of the Research Vessel 'Polarstern' to the Antarctic in 2003 (ANT-XXI/1)", edited by Otto Schrems

Heft-Nr. 606/2010 — "The Expedition of the Research Vessel 'Polarstern' to the Antarctic in 2008 (ANT-XXIV/3)", edited by Eberhard Fahrbach and Hein de Baar

Heft-Nr. 607/2010 — "The Expedition of the Research Vessel 'Polarstern' to the Arctic in 2009 (ARK-XXIV/2)", edited by Michael Klages

Heft-Nr. 608/2010 — "Airborne lidar observations of tropospheric Arctic clouds", by Astrid Lampert

Heft-Nr. 609/2010 — "Daten statt Sensationen - Der Weg zur internationalen Polarforschung aus einer deutschen Perspektive", by Reinhard A. Krause

Heft-Nr. 610/2010 — "Biology of meso- and bathypelagic chaetognaths in the Southern Ocean", by Svenja Kruse

Heft-Nr. 611/2010 — "Materialparameter zur Beschreibung des zeitabhängigen nichtlinearen Spannungs – Verformungsverhaltens von Firn in Abhängigkeit von seiner Dichte", by Karl-Heinz BäSSLer

Heft-Nr. 612/2010 — "The Expedition of the Research Vessel 'Polarstern' to the Arctic in 2009 (ARK-XXIV/1)", edited by Gereon Budéus

Heft-Nr. 613/2010 — "The Expedition of the Research Vessel 'Polarstern' to the Antarctic in 2009 (ANT-XXV/3 - LOHAFEX)", edited by Victor Smetacek and Syed Wajih A. Naqvi

Heft-Nr. 614/2010 — "The Expedition of the Research Vessel 'Polarstern' to the Antarctic in 2009 (ANT-XXVI/1)", edited by Saad el Nagggar and Andreas Macke